HHS Public Access

Author manuscript

Sci Signal. Author manuscript; available in PMC 2016 December 07.

Published in final edited form as:

Sci Signal. ; 9(454): ra111. doi:10.1126/scisignal.aaf6670.

RasGRP1 promotes amphetamine-induced motor behavior through a Rhes interaction network ("Rhesactome") in the striatum**

Neelam Shahani[1], **Supriya Swarnkar**[1], **Vincenzo Giovinazzo**[1], **Jenny Morgenweck**[2], **Laura M. Bohn**[2], **Catherina Scharager-Tapia**[3], **Bruce Pascal**[4], **Pablo Martinez-Acedo**[3], **Kshitij Khare**[5], and **Srinivasa Subramaniam**[1,*]

[1]Department of Neuroscience, The Scripps Research Institute, Jupiter, Florida 33458. USA.

[2]Department of Molecular Therapeutics, The Scripps Research Institute, Jupiter, Florida 33458. USA.

[3]Proteomics Core, The Scripps Research Institute, Jupiter, Florida 33458. USA.

[4]Informatics Core, The Scripps Research Institute, Jupiter, Florida 33458. USA.

[5]Department of Statistics, University of Florida, Gainesville, FL 32611. USA.

Abstract

The striatum of the brain coordinates motor function. Dopamine-related drugs may be therapeutic to patients with striatal neurodegeneration, such as Huntington's disease (HD) and Parkinson's disease (PD), but these drugs have unwanted side effects. In addition to stimulating the release of norepinephrine, amphetamines, which are used for narcolepsy and hyperactivity disorder (ADHD), trigger dopamine release in the striatum. The GTPase Ras homolog-enriched in the striatum (Rhes) inhibits dopaminergic signaling in the striatum, is implicated in HD, and has a role in striatal motor control. We found that the guanine nucleotide exchange factor (GEF) RasGRP1 inhibited Rhes-mediated control of striatal motor activity in mice. RasGRP1 stabilized Rhes, increasing its synaptic accumulation in cultured striatal neurons.. Whereas partially Rhes-deficient (*Rhes*$^{+/-}$) mice had an enhanced locomotor response to amphetamine, this phenotype was attenuated by coincident depletion of RasGRP1. By proteomic analysis of striatal lysates from *Rhes*-heterozygous mice with wild-type or partial or complete knockout of *Rasgrp1*, we identified a diverse set of Rhes-interacting proteins, the "Rhesactome," and determined that RasGRP1

*To whom the correspondence should be addressed: Srinivasa Subramaniam, Department of Neuroscience. The Scripps Research Institute, Jupiter, Florida 33458. USA Tel: 561-228-2104; Fax: 561-228-2107; ssubrama@scripps.edu.

Author contributions: N.S. designed, performed behavioral, biochemical experiments and all related data analysis and contributed to the bioinformatics analysis. S. Swarnkar carried out overexpression studies. V.G performed cyclohexamide experiments and genotyping the mice. J.M. and L.M.B. contributed to amphetamine behavioral work, P.M.-A. C.S.-T. carried out LCMS/MS and data analysis, B.P performed bioinformatics and related data analysis. K.K. contributed to statistical analysis and its validation. S. Subramaniam conceptualized the project and co-designed the experiments, and wrote the papers with the input from the co-authors.

Data and materials availability: The complete data set from the analysis of the "Rhesactome" (raw files, identification data and data analysis files) is available in the PeptideAtlas repository (http://www.peptideatlas.org/PASS/PASS00940) that can be downloaded via ftp://PASS00940:TF4767qx@ftp.peptideatlas.org/ .

affected the composition of the amphetamine-induced Rhesactome, which included PDE2A (phosphodiesterase 2A, a protein associated with major depressive disorder), LRRC7 (leucine-rich repeat-containing 7, a protein associated with PD and ADHD), and DLG2 (disks large homolog 2, a protein associated with chronic pain). Thus, this Rhes network provides insight into striatal effects of amphetamine and may aid the development of strategies to treat various neurological and psychological disorders associated with the striatal dysfunction.

INTRODUCTION

The striatum serves as a central hub to regulate the motor, psychiatric, and cognitive functions of the brain (1). Dopamine, produced mainly from projection neurons in the substantia nigra pars reticulata (SNc), is believed to exert its primary actions in the medium-spiny neurons (MSNs) of the striatum by acting on dopamine receptors (2). Glutamate (Glu), produced from projection neurons in the cortex acts through ionotropic [N-Methyl-D-aspartate (NMDA) or α-amino-3-hydroxy-5-methyl-4-isoxazolepropionic acid (AMPA) receptors. In addition to these, there are abundant acetylcholine and serotonergic inputs to MSNs, but how these different receptors coordinate as a microcircuit in the striatum, and how they promote motor-signaling, remains less well understood (3, 4). Dysregulation of dopamine signaling promotes movement disorders, such as dystonia, Huntington's disease (HD) and Parkinson's disease (PD). Whereas HD motor symptoms, characterized by hyperkinetic movements, occur due to the degeneration of MSNs, PD motor symptoms, such as lack of initiation of movements occurs due to degeneration of SNc neurons. Agents that prevent the degeneration of these neurons are currently not available. Dopamine-related drugs such as tetrabenazine and L-DOPA reduce hyperkinetic movement in HD and correct the hypokinetic movements in PD, respectively. However, prolonged administration of these drugs may elicit abnormal motor side effects (5, 6). Therefore, there is an urgent need to understand the dopaminergic-signaling mechanisms within the striatum, not only from a basic biology point of view, but also to help refine therapeutic agents to treat movement disorders.

Rhes is a guanosine triphosphatase (GTPase) that is highly abundant in the MSNs of the striatum (7), and we have previously discovered that it has a small-ubiquitin-like modifier (SUMO) E3 ligase activity and plays a crucial role in the pathogenesis of HD in cell culture and in mouse models (8-11), a finding also supported by several independent studies (12-17). Moreover, we found that Rhes binds to and activates the mammalian target of rapamycin (mTOR), in a GTP-dependent manner, which plays a crucial role in the generation of L-DOPA-induced dyskinesia in a PD pre-clinical mouse model (18), a finding recently confirmed by another study (19). *Rhes* knockout (KO) mice are fertile and have no obvious gross phenotype; however, they do exhibit enhanced behavioral responses to psychostimulants and dopamine receptor ligands compared to wild-type mice (20-23). For example, *Rhes* KO mice exhibit greater locomotion compared to wild-type mice in response to the dopamine D1 agonists SKF8127 or amphetamine (20, 24) and an increased catalepsy in response to the dopamine D2 antagonist haloperidol (23). Despite these studies, the mechanism that enables Rhes to exert such inhibitory effects on dopaminergic signaling in the striatum is not yet clear.

RAS guanyl releasing protein 1 (RasGRP1, also known as CalDAG-GEFII) is a guanine-nucleotide exchange factor (GEF) for H-Ras that activates extracellular-signal regulated kinase (ERK) (25-27). The Graybiel group found that RasGRP1 is highly expressed in the striatum and is strongly upregulated in a dyskinesia model of PD (27, 28). RasGRP1 is also expressed in hematopoietic cells and has been implicated in leukemia and lupus (29-33). Here, using a hypothesis-driven as well as a genetic, behavioral, and high-throughput approach, we investigated the role of RasGRP1 in the striatum and found that RasGRP1 interacts with Rhes to regulate striatal control of motor functions.

RESULTS

RasGRP1 interacts with Rhes in the striatum

To identify potential regulators of Rhes, we tested whether co-transfection of the striatal-enriched GEF, His-tagged RasGRP1, together with myc-tagged Rhes, could alter the mTOR and MEK-ERK signaling pathway in mouse striatal neuronal cells and human embryonic kidney 293 (HEK293) cells. We found that expression of His-RasGRP1 and myc-Rhes together promoted activation of mTOR and MEK-ERK signaling, compared to expression of either alone, as measured by Western blotting analysis of the phosphorylation of S6 and ERK, respectively, both in murine striatal and HEK293 cells (**Fig. 1A**). The protein abundance of myc-Rhes in cells coexpressing His-RasGRP1 was several-fold higher than that in cells transfected with myc-Rhes alone, suggesting that RasGRP1 might physiologically regulate the protein abundance of Rhes. To test this, we carried out Western blotting analysis of endogenous Rhes protein in striatal tissue from *Rasgrp1*$^{-/-}$ mice. Rhes physiologically exist in three different forms, the native −32 kDa, or modified or alternatively spliced −39 or −47 kDa forms, as seen in previous reports (8, 11, 34, 35). We found that the Rhes abundance was −25% significantly reduced in *Rasgrp1*$^{-/-}$ mice striatum compared to wild-type mice (**Fig. 1B**). These Rhes bands were absent in *Rhes*$^{-/-}$ mice striatum, as expected **(Fig. 1B)**. We further confirmed that the −47 kDa higher mobility band (**Fig. 1B**) was indeed Rhes protein by immunoprecipitation (IP) and liquid chromatography-mass spectroscopy (LC-MS/MS) analyses (**fig. S1**). A further reduction of Rhes was not apparent in heterozygous mice, the *Rhes*$^{+/-}$/*Rasgrp1*$^{-/-}$ (**fig. S2**), suggesting that RasGRP1 partially controls the stability of endogenous Rhes at or above a certain critical abundance or at a particular intracellular location in the striatum.

To look into these possibilities, we investigated whether RasGRP1 alters the half-life of myc-Rhes, using cyclohexamide (CHX) chase experiment. To our surprise, myc-Rhes is a very stable protein and its half-life seems to be beyond the 32-hour window analyzed (fig. S3). Whereas myc-Rhes abundance was expectedly enhanced by His-RasGRP1 coexpression, its abundance was not reduced even after 32 hours with CHX. However, that of endogenous Rheb, endogenous β-secretase (BACE1), and His-RasGRP1 were markedly reduced by half or more below that in the starting condition. This suggests that Rhes is a relatively stable protein, but the mechanisms involved are unclear. To test whether RasGRP1 alters the intracellular localization of Rhes, we carried out a biochemical organelle separation, and found that myc-Rhes robustly accumulated in the membrane fraction in the presence of excess HisRasGRP1 (**fig. S4AB**). Next, we reasoned that RasGRP1 might

physiologically alter localization of Rhes in the striatum. Biochemical subcellular fractionation of striatal tissue revealed that Rhes protein abundance are reduced selectively in the synaptosomal fractions of the *Rasgrp1*$^{-/-}$ mice striatum, compared to wild-type mice (**Fig. 1C**). However, there were no significant changes in Rhes protein abundance in the cytosolic fractions between the genotypes. The abundance of PSD-95, a synaptic marker, was not different between the wild-type and *Rasgrp1*$^{-/-}$ mice.

Because RasGRP1 physiologically promotes the protein abundance and synaptic associations of Rhes, we then investigated whether they interact. In striatal brain lysate, the endogenous RasGRP1, but not DARPP-32, an abundant striatal protein, binds to GST-Rhes (**Fig. 1D**). mTOR, which we determined previously to interact with Rhes (18), also binds to GST-Rhes, as expected. To determine whether the interaction of RasGRP1 and Rhes can occur in the striatum, we performed an endogenous Co-IP experiment with Rhes IgG (8). First, we further validated whether the Rhes antibody works in IP using LC-MS/MS and *Rhes*$^{-/-}$ control. IP of endogenous Rhes from wild-type mice striatal lysate, using Rhes IgG, but not control IgG, revealed enrichment of the Rhes peptide in LC-MS/MS analysis (**fig. S5**). As expected, IP using Rhes IgG in *Rhes*$^{-/-}$ mice did not detect any Rhes peptide (**fig. S5**), suggesting that the Rhes IgG used in this study is very specific to Rhes. A Co-IP experiment using this validated Rhes IgG revealed a physiological interaction of endogenous Rhes with endogenous RasGRP1 in the striatum (**Fig. 1E**). We also confirmed that Rhes physiologically interacted with mTOR in the striatum (**Fig. 1E**). RasGRP1 interaction is dependent on Rhes Cys^{263}, a potential farnesylation site, its mutation mislocalizes Rhes predominantly to the nucleus (8), and the interaction is greatly diminished by the consensus GTP/GDP binding mutants of Rhes (D143N, nucleotide free; G31V, GDP-bound; S33N, GDP-bound) (**fig. S6**). We found that this interaction is direct, as purified RasGRP1 bound to Rhes, independent of GTP in vitro (**Fig. 1F**). Domain-binding experiments demonstrated that the N-terminal sequence of GST-Rhes, spanning 1-135 amino acids, and the C-terminal 141-266 amino acid sequence both bound strongly to His-RasGRP1 (**Fig. 1, G** and **H**). Previous studies showed the GEFs, such as SOS, C3G, CalDAG-GEF3, or RasGRP2, had no detectable GEF activity toward purified recombinant Rhes (36). Because we found a direct interaction between RasGRP1 and Rhes, we tested whether RasGRP1 can act as a GEF for Rhes and found that RasGRP1 significantly increased GTP loading, using a [^{35}S]GTPγS filter-binding assay, an effect that is comparable to H-Ras (**Fig. 1I**). Altogether, these data suggest that (i) Rasgrp1 promotes the protein abundance of Rhes and its synaptic association in the striatum, and (ii) Rasgrp1 directly binds to Rhes in the striatum and acts like a GEF for recombinant Rhes.

RasGRP1 inhibits Rhes to promote amphetamine-induced motor activity

Having established that RasGRP1 biochemically interacts with and promotes the abundance of Rhes; we hypothesized that this strong biochemical association might have a functional relevance in regulating the striatal behaviors. To test this, we adopted an amphetamine-induced behavioral activity model. The psychostimulant amphetamine acts at dopamine transporters to increase levels of extracellular dopamine, which acts on striatal post-synaptic dopamine receptors leading to stimulation of locomotor behaviors (37-43). Acute intraperitoneal (i.p) injection of amphetamine (2 mg/kg, at 10 μl/g, dissolved in 0.9% saline)

resulted in a robust increase of locomotor activity (distance traveled) and stereotypy (repeated beam breaks) in *Rhes*$^{-/-}$ but not wild-type mice (**Fig. 2, A-D**; n=4-6 mice/group, mixed sex ratio). Because 2 mg/kg i.p. injection of amphetamine did not elicit any response in wild-type mice, we increased the dose of amphetamine to 3 mg/kg in *Rhes*$^{-/-}$ mice, which produced greater locomotor activity and stereotypy response relative to wild-type controls, which showed a slight but significant increase in locomotion and a slight decrease in stereotypic behaviors (**Fig. 2, E-H,** n = 8/group, mixed sex ratio), consistent with a previous report (44). The basal (spontaneous) locomotor activity before amphetamine administration appeared similar in both wild-type and *Rhes*$^{-/-}$ mice (**Fig. 2, A, B, E, and F**).

To investigate whether—and if so, how—RasGRP1 influences Rhes in amphetamine-induced behavioral activity, we bred single and double mutants of *Rasgrp1* and *Rhes*, and found that they displayed differential effects on amphetamine-induced locomotion and stereotypy response. Whereas amphetamine injection into the peritoneum (3 mg/kg at 10 μl/g) increased both locomotor activity and stereotypic behaviors in single knockout (KO) *Rhes*$^{-/-}$ mice (**Fig. 2, A-G)**, it had differential motor behavioral effects in single KO *Rasgrp1*$^{-/-}$ mice. Locomotor activity in *Rasgrp1*$^{-/-}$ mice was similar to that in wild-type controls, and the emergence of stereotypic behaviors was delayed (~15 min after amphetamine injection) (**Fig. 2, I-L;** n=6-7 mice/group, mixed sex ratio). Double KO (*Rhes*$^{-/-}$*/Rasgrp1*$^{-/-}$) mice, however, showed significantly greater locomotor activity than single KO (*Rhes*$^{-/-}$) mice and displayed stereotypic behaviors similar to that of the single KO *Rhes*$^{-/-}$ mice (**Fig. 2, I-L;** n=6-7 mice/group, mixed sex ratio). Together, these behavioral studies in homozygous KO mice suggest that (i) loss of Rhes increases amphetamine-induced motor behaviors, suggesting that Rhes acts as an inhibitor of amphetamine-induced motor behaviors; (ii) loss of RasGRP1 does not elicit any significant effect on amphetamine-induced motor behaviors; and (iii) loss of both RasGRP1 and Rhes exacerbates amphetamine-induced locomotion, suggesting these two protein interact to inhibit striatal motor functions.

Although a complete ablation of *Rasgrp1* or *Rhes* offered important insights about their loss of a functional role in striatal motor behaviors, we reasoned that the heterozygous mutant mice with reduced (but not abolished) RasGRP1 or Rhes protein abundance could provide physiological information about how these proteins interact during amphetamine-induced behavior. Moreover, the use of heterozygous mice would potentially avoid the influence of any compensatory pathways in the observed phenotype. Therefore, we evaluated the effects of amphetamine (3 mg/kg at 10 μl/g) injected into the peritoneum of heterozygous mice (*Rhes*$^{+/-}$*/Rasgrp1*$^{+/+}$, *Rhes*$^{+/-}$*/Rasgrp1*$^{+/-}$, *Rhes*$^{+/-}$*/Rasgrp1*$^{-/-}$, n=6-8 mice/group, mixed sex ratio*).* Consistent with behavioral data in homozygous *Rhes* KO mice (*Rhes*$^{-/-}$, **Fig. 2, E-H**), we found that heterozygous Rhes mice (*Rhes*$^{+/-}$*/Rasgrp1*$^{+/+}$) are hyperactive in response to amphetamine (locomotion and stereotypic behaviors) compared to wild-type controls (**Fig. 2, M-P**). However, *Rhes*$^{+/-}$ mice that are also partially depleted of RasGRP1 (*Rhes*$^{+/-}$/*Rasgrp1*$^{-/-}$), showed a strongly attenuated response to amphetamine-induced locomotion or stereotypic behaviors. Based on these data, we propose that decreasing the levels of RasGRP1 makes Rhes highly inhibitory, and therefore, the loss of RasGRP1 may have a dose-dependent effect on blocking amphetamine-induced motor behavior. Consistent with

this notion, although mice with homozygous deletion of RasGRP1 (*Rhes*$^{+/-}$/*Rasgrp1*$^{-/-}$) appeared to be phenotypically closer to wild-type littermate controls, mice with heterozygous deletion of RasGRP1 (*Rhes*$^{+/-}$/*Rasgrp1*$^{+/-}$) displayed a significantly higher sensitivity compared to wild-type controls, albeit less sensitively than *Rhes*$^{+/-}$/*Rasgrp1*$^{+/+}$ mice (**Fig. 2, M-P**). Together, these data suggest that Rhes physiologically inhibits motor activity, and that RasGRP1 exerts an inhibitory control over Rhes thus disinhibiting it from blocking motor behavior.

Amphetamine elicits a "Rhesactome," a previously unknown Rhes protein network in the striatum

To study the potential neuronal mechanisms by which RasGRP1 and Rhes regulate amphetamine-induced motor behavior, we took unbiased systems biology approach. We hypothesized that Rhes-mediated inhibitory control over motor behavior in the striatum involves the formation of a dynamic protein complex network. To test this, we reasoned that capturing the *in vivo* protein interaction of Rhes during amphetamine injection would provide a better understanding of the mechanisms of how Rhes functions as a suppressor of drug-induced motor behavior in the striatum. To accomplish this, we injected amphetamine (3 mg/kg at 10 μl/g) into the peritoneum of wild-type mice, and after 15 minutes (at which time the mice reached maximum locomotion/stereotypy) the striatum was isolated and its protein lysates were subjected to IP using a relatively specific Rhes IgG (**fig. S5**) or control IgG, followed by LC-MS/MS analysis (**fig. S7)**. To ensure high confidence in our interactome data, we used two types of controls in IP/LC-MS/MS analysis: i) control IgG-incubated wild-type mice striatal lysate; and ii) Rhes IgG-incubated *Rhes* KO striatal lysate, to rule out the tendency of Rhes IgG to cross-react with "secondary" antigens (**fig. S7).** List of all proteins ($\log_2$ fold change) identified in control IgG IP LC-MS/MS in the wild-type mice striatum (Control 1) or Rhes IgG IP LCMS/MS in the *Rhes*$^{-/-}$ mice striatum (Control 2), in amphetamine vs. saline conditions (3 mg/kg i.p. at 10 μl/g) is provided in the supplementary information **(Data files S3 and S4)**. The specific Rhes interactors were derived from the subtraction of the IP/LC-MS/MS results from controls thus increasing the confidence of our interaction proteomics (the number of mice per IP per group is indicated in **table S1)**. Scaffold peptide identifications carried at 1% FDR revealed 303 Rhes protein interactors in saline (basal) conditions and 351 interactors in amphetamine-treated conditions, collectively termed as "Rhesactome." A Venn analysis revealed there were 282 Rhes interacting proteins present in both conditions, 21 proteins were unique to basal condition and 69 proteins were unique to amphetamine condition (**Fig. 3A).** We further validated a few Rhes interactors (Syngap1, Rgs9, Kif5c) in an IP-Western blot assay (**fig. S8**). The individual role of the Rhes interactors (**Fig. 3B**) in Rhes-mediated striatal functions requires further exploration.

To further analyze, understand, and model the "Rhesactome" with respect to the amphetamine-induced behavioral response, we used ingenuity pathway analysis (IPA) and STRING interaction bioinformatics. IPA bioinformatics found that the "Rhesactome" consists of proteins associated with six major pathways and five biofunctions (**Fig. 3C**). While both saline and amphetamine conditions shared pathways belongs to EIF2 signaling, mTOR signaling, and eIF4 and p70S6K signaling, GNRH signaling was restricted to saline,

and whereas protein kinase A and clathrin-mediated endocytosis signaling was restricted to amphetamine condition. Similarly, while both conditions shared the proteins associated to biological functions such as cell death and survival (**Fig. 3C**), the proteins associated with RNA post-transcriptional modification was present only in amphetamine condition.

Using STRING database we curated the known and predicted protein interactions in "Rhesactome," that are enriched in amphetamine, compared to saline, or present exclusively in amphetamine conditions (**Fig. 3, D and E)**. Proteins involved in translation and pre-mRNA processing are the two major categories that are enriched in amphetamine conditions (**Fig. 3D**), but for most other proteins that interacted with Rhes exclusively in amphetamine condition, the functional or physical interactions are currently unknown (**Fig. 3E**). This suggests that a certain set of new proteins associate with, and dissociate from, Rhes, only in amphetamine condition, that may have a major role in promoting the motor functions regulated by the striatum. Thus, by adopting an intended unbiased approach and stringent antibody and tissue controls, we discovered a highly specific striatal "Rhesactome" under basal and amphetamine conditions in the striatum. A complete list of the specific striatal proteins ($\log_2$ fold change) bound to Rhes in amphetamine compared to saline conditions from wild-type mice is provided in the supplementary information (**Data file S1**).

RasGRP1 promotes "Rhesactome" formation in the striatum

Because RasGRP1 controls the hyperactive phenotype in *Rhes*$^{+/-}$/*Rasgrp1*$^{+/+}$ mice (**Fig. 2, M-P**), we reasoned that the RasGRP1 might regulate the formation of the amphetamine-induced "Rhesactome" in the striatum. To test this assumption, we performed IP/LC-MS/MS analysis of Rhes interactors from RasGRP1 intact mice **(***Rhes*$^{+/-}$/*Rasgrp1*$^{+/+}$), and RasGRP1 KO mice (*Rhes*$^{+/-}$/*Rasgrp1*$^{-/-}$) upon intraperitoneal injection of amphetamine (3 mg/kg at 10 μl/g; the number of mice per IP per group is indicated in **table S1**). Proteomics analysis (at 1% FDR) identified 217 Rhes protein interactors in amphetamine-injected *Rasgrp1* intact mice (*Rhes*$^{+/-}$/*Rasgrp1*$^{+/+}$) and only 145 interactors in the mice that lacked *Rasgrp1* (*Rhes*$^{+/-}$/*Rasgrp1*$^{-/-}$) (**Fig. 4A**). A Venn analysis revealed there were 103 Rhes interacting proteins present in both genotypes, 114 proteins were unique to *Rhes*$^{+/-}$/*Rasgrp1*$^{+/+}$ mice and 42 proteins were unique to *Rhes*$^{+/-}$/*Rasgrp1*$^{-/-}$ mice (**Fig. 4A**). A selected list of Rhes interacting proteins ($\log_2$ fold change) (**Fig 4B)** shows (i) Rhes interacting proteins absent in *Rhes*$^{+/-}$/*Rasgrp1*$^{-/-}$ mice striatum compared to *Rhes*$^{+/-}$/*Rasgrp1*$^{+/+}$; (ii) Rhes interacting proteins altered in *Rhes*$^{+/-}$/*Rasgrp1*$^{-/-}$ mice striatum compared to *Rhes*$^{+/-}$/ *Rasgrp1*$^{+/+}$; and (iii) Rhes interacting proteins found only in *Rhes*$^{+/-}$/*Rasgrp1*$^{-/-}$ mice striatum compared to *Rhes*$^{+/-}$/*Rasgrp1*$^{+/+}$. IPA bioinformatics found that the "Rhesactome" in both the genotypes consists of proteins associated with six major pathways and biological functions (**Fig. 4C**). While the "Rhesactome" of *Rhes*$^{+/-}$/*Rasgrp1*$^{+/+}$ consisted of proteins associated with IL-1 signaling, adrenergic signaling, cell morphology and development, they were absent in the "Rhesactome" of *Rhes*$^{+/-}$/*Rasgrp1*$^{-/-}$ mice striatum. Conversely, the "Rhesactome" of *Rhes*$^{+/-}$ /*Rasgrp1*$^{-/-}$ consisted of proteins implicated in cell junction, gene expression and translation but they were absent in the "Rhesactome" of *Rhes*$^{+/-}$/*Rasgrp1*$^{+/+}$ mice. This suggests that lack of RasGRP1 results in either absent or diminished formation of the "Rhesactome" in the striatum. Some of the previously documented or related Rhes or RasGRP1 interactors were found in "Rhesactome." (**table S2**). A complete list of all the

Rhes interactors in *Rhes*$^{+/-}$/*Rasgrp1*$^{+/+}$ and *Rhes*$^{+/-}$/*Rasgrp1*$^{-/-}$ mice striatum is indicated in the (**Data file S2**).

Overall, based on biochemical, genetic, and behavioral interactions of RasGRP1 and Rhes, as described above, we propose a model (**Fig. 4D**) wherein RasGRP1 exerts inhibitory control over Rhes through a "Rhesactome" that prevents Rhes from inhibiting amphetamine-induced mechanisms underlying motor behavior (I). Thus haploinsufficiency or homozygous deletion of *Rasgrp1* reduces its inhibition over Rhes, thereby enhancing the inhibitory activity of Rhes and suppressing the motor response to amphetamine (II and III). Overall RasGRP1 disinhibits Rhes to promote motor response to amphetamine through "Rhesactome" protein network in the striatum. Our observation of higher motor activity in double-knockout mice in response to amphetamine compared to either single knockout mouse lines suggests that RasGRP1 has additional (non-Rhes) targets that are yet to be discovered.

DISCUSSION

Despite many advances, the precise striatal signaling mechanisms that regulate motor functions remains less clear (45-47). Here, we found that RasGRP1-Rhes signaling circuitry modulates striatal motor functions. On the basis of the behavioral activity model of amphetamine, which increases extracellular dopamine at dopaminergic terminals and dendrites in the striatum (38, 48, 49), we predict that striatal Rhes physiologically inhibits dopaminergic signaling in the striatum. Our study is consistent with previous studies implying Rhes as an inhibitor of dopaminergic signaling in the striatum (20, 22, 50, 51) but which lacked clear mechanisms. We found that through modulating the "Rhesactome," a dynamic Rhes-interaction signaling network in the striatum, RasGRP1 acts as a physiological inhibitor of Rhes to promote motor activity and response to amphetamine. Our model predicts that Rhes physiologically inhibits motor activity, and certain protein partners in the Rhesactome induced by amphetamine inhibits Rhes, thereby eliciting motor activity. Mechanistically, how or whether protein partners in the "Rhesactome" inhibits Rhes or vice-versa, or whether these two possibilities are mutually inclusive, is unclear. Nevertheless, our "Rhesactome" reveals interesting binding-partners of Rhes. For example, PDE1B, SHANK3 and FMR1 (Data file S1), which are implicated in regulating the hyperactive phenotype in response to amphetamine (52-54), in association with Rhes may regulate inhibitory motor control in the striatum. Based on the interaction data, we predict multiple mechanisms involved in Rhes-mediated inhibition. For example, it might involve the AKT pathway. Beaulieu and colleagues showed that amphetamine reduces AKT activation, which occurs through the formation of β-arrestin/protein phosphatase 2A/AKT complexes leading to the activation of motor activity (55, 56). Because Rhes can also regulate AKT (35, 57) and binds to arrestin (S-arrestin) and protein phosphatase (Ppp1cc) (Data file S1), the involvement of these proteins in Rhes–AKT signaling to inhibit motor function cannot be ruled out. Rhes can also diminish motor activity by enhancing the dopamine receptors internalization through clathrin-mediated endocytic pathway as it binds to the several components of this pathway, including clathrin, AP2S1, Rab11, Arf5, and PIP5k1c (58-60) (Data file S1). The detailed mechanisms herein remain to be determined.

The striatum predominantly comprises dopamine D1 and D2 receptor positive MSN, which have multiple inputs and outputs, and their inherently complex interactions promote striatal behaviors, which includes cognitive and psychiatric functions. RasGRP1 and Rhes are present in both dopamine D1 and D2 receptor-positive MSN, and thus, we predict that the "Rhesactome" is downstream of dopamine D1 or D2 receptor signaling, comprised predominantly of postsynaptic, nuclear, and some pre-synaptic complexes. In addition to dopaminergic inputs from SNc, some major inputs include: GABAergic inputs from the globus pallidus, and glutamatergic inputs from corticostriatal and subthalamic nucleus. Whether or how RasGRP1 and Rhes signaling participate with this different striatal inputs is currently unknown. Because Rhes and RasGRP1 are also present to some extent in the cortex of the brain (24, 27), their involvement in cortical-striatal signaling is plausible.

This study raises another interesting question: What are the mechanisms by which RasGRP1 mediate the "Rhesactome" formation in the striatum? Based on our biochemical data, we speculate that RasGRP1 promotes the synaptic accumulation of Rhes to facilitate the "Rhesactome" formation. Because Rhes is also localized to vesicles, the trans-Golgi and the nucleus (fig. S4C), the possibility of inhibitory action occurring through multiple locations, including transcriptional mechanisms (61) cannot be excluded. A major challenge is to address the striatal role of the components of the "Rhesactome." Considering that Rhes is a physiological regulator of SUMOylation (9), which is known to regulate diverse molecular functions, such as localization, stability, gene transcription, and protein-protein interactions (62), it would be interesting to analyze what role SUMOylation plays in the formation of the "Rhesactome" and in motor behaviors.

What remains unknown at this point is how RasGRP1 modulates Rhes abundance. We speculate that both transcriptional and posttranscriptional mechanisms are involved. Feedback regulation via enhanced ERK or mTOR signaling, which are well-known regulators of transcription and translation, might increase the abundance of Rhes in the striatum. Considering Rhes protein abundance is enhanced predominantly at synaptic locations, we predict an intriguing possibility that RasGRP1 regulate local translation of *Rhes* mRNA at the synapse.

The significance of this study can also be applicable on many fronts. Inhibitory controls play a fundamental role in living organisms, and deficits in those control mechanisms promote impulsive actions, which are the hallmark of many striatal-associated diseases, such as HD, PD, attention deficit hyperactivity disorder, bipolar disorder, schizophrenia, and addiction behaviors (63-68). Moreover, some studies have shown a causal link for Rhes and RasGRP1 in some of these disorders. For example, recent studies have suggested a genetic variation in the *Rhes* and *Rasgrp1* gene as a contributory factor in a subgroup of schizophrenia and bipolar disorder, respectively (24, 69-71). Although the role of RasGRP1 in addiction behavior is unknown, Rhes regulates enhanced analgesia, diminished tolerance, and withdrawal from morphine (23). Similarly, there is a biochemical association of RasGRP1 and Rhes in L-DOPA-induced dyskinesia (LID), an abnormal motor coordination due to deregulated striatal dopamine signaling, which affects a vast majority of PD patients under L-DOPA medication. Striatal signaling, including the ERK, mTORC1, and dopamine D1/D2 receptor pathways, orchestrates LID (72). Earlier, we demonstrated that Rhes activates

mTORC1 signaling, and there is partial alleviation of LID in *Rhes* KO mice (18). The present study reveals that RasGRP1 and Rhes potentiate both ERK and mTORC1 signaling and that the mTOR pathway is one of the top pathways in the “Rhesactome”. Therefore, we predict that RasGRP1, the gene expression and protein abundance of which is upregulated during dopamine signaling in LID (28), together with Rhes, can potentiate the abnormal motor movements of LID in PD., In animal models of HD, Rhes promotes motor, psychiatric-like, and anatomical deficits (11, 23), but whether and how RasGRP1 participates in HD remains to be determined.

The findings also have clinical implication for amphetamine-related therapy and disorders (73). Although amphetamine and related drugs are prescribed to treat children, adolescents, or adults diagnosed with narcolepsy and attention deficit disorders, it is a potent but dangerous psychostimulant with a high risk for abuse and addiction, placing it among one of the world's fastest growing illicit drugs (74, 75). Besides enhancing a complex dopaminergic signaling, how amphetamine-induced downstream signaling is orchestrated in the striatum requires more studies (76, 77). Chronic abuse of methamphetamine is associated with abnormally high striatal activity (measured by glucose metabolism) and an enlargement of striatal volume in the adult human (78), a phenomenon implicated as an adaptive response and/or a predisposing factor to amphetamine abuse (75). A recent genome-wide association study predicts that the single nucleotide polymorphisms might contribute to the differential sensitivity among individual human to amphetamine (79), suggesting that the mechanisms of amphetamine action are more complex than simply altering dopamine concentrations in the striatum. Amphetamine regulates expression of several genes, such as those, which encode brain-derived neurotrophic factor (BDNF), and the transcription factors c-Fos and Zif268, in the striatum (80-83). Pharmacological and genetic studies have revealed the role of dopamine- and glutamate-related signaling molecules in the amphetamine-induced behavioral response. For example, antagonists of dopamine receptors (D1R or D2R) or NMDA receptor, or a genetic deficiency in CAMKIIα, β-arrestin, GSK-3β, or the adenosine receptor, attenuate the amphetamine-induced response in mouse models, whereas an overexpression of dopamine transporter in the striatum or a deficiency in protein kinase A enhances the behavioral response to amphetamine (55, 56, 84-87). Many of these molecules are expressed in diverse areas of the brain (2, 88-91), and whether or how they regulate amphetamine signaling selectively in the striatum in association with “Rhesactome” remains to be determined. Such studies might provide deeper molecular insights into how striatal-specific regulators modulate the therapeutic versus addictive properties of amphetamine.

In summary, using a combination of genetic, behavioral, and proteomics approaches we have demonstrated how two striatal-enriched proteins, RasGRP1 and Rhes, operate through a protein-protein interaction network – a “Rhesactome” – in the striatum during motor stimuli, which may have broader implications in neurological, psychiatric, and addictive disorders. Therefore, drugs that bind RasGRP1 and/or Rhes may have therapeutic benefits for the diseases that affect striatum.

MATERIALS AND METHODS

Reagents, Plasmids, and Antibodies

Chemicals and reagents were mainly purchased from Sigma. Myc-tagged Rhes wild-type and S33N, D143N, and C263S, and all the other indicated Rhes deletion mutants expressing cDNA constructs were prepared as described previously (8, 18). His-tagged rat RasGRP1 was a gift from Ann Graybiel (MIT). The myc-tagged RasGRP1 (pCMV-myc) and GST-tagged (pGEX-6P2) RasGRP1 constructs were produced from a His-RasGRP1 construct. Antibodies for RasGRP1, GST-HRP, and Myc were obtained from Santa Cruz (SC8430, SC138, and SC40, respectively). His antibody was from Sigma (H1029). Antibodies for RasGRP1 (clone 10.1) and Rhes were obtained from Millipore (MABS146 and ABN31, respectively). Antibodies against mTOR (2972S), pS6K T389 (9234S), pS6 S235/236 (4858S), p44/42 ERK1/2 T202/Y204 (9101S), S6K (9202S), S6 (2217S), ERK1/2 (4695P), EEA1 (3288S), Syntaxin 6 (2869S), Calnexin (2679S), and DARPP-32 (2302S) were from Cell Signaling Technology. Rgs-9 antibody was a gift from Kirill Martemyanov, kif5c antibody was from Sathya Puthanveettil, and syngap1 antibody was from Gavin Rumbaugh. Glutathione beads were from Amersham Biosciences and Protein G/Protein A agarose beads were obtained from Calbiochem. Nuclear/Cytosol Fractionation Kit was from BioVision Inc.

Cell Culture, and Transfections

Striatal neurons (from *STHdh*$^{Q7/Q7}$ mice) or HEK293 cells were cultured in growth medium containing DMEM (Gibco 11965-092) with 10% FBS (fetal bovine serum), 1% pen strep, and 5 mM glutamine, essentially as described before (8, 10). Cells seeded in 3.5- or 6-cm plates were transfected 24 hours later with cDNA constructs using polyfect (Qiagen) as per the manufacturer's instructions.

Western blotting and Immunoprecipitation experiments

Western blotting and glutathione-binding experiments were followed as described previously (8, 98). Briefly, GST or GST-Rhes or GST-Rhes fragments or His-RasGRP1 or myc-Rhes (1 μg each) were transfected in striatal or HEK293 cells, and, after 48 hr, cells were lysed in lysis/binding buffer (50 mM Tris, pH 8.0, 150 mM NaCl, 10%glycerol, 1.0% NP-40) with a protease inhibitor cocktail (Roche) and phosphatase inhibitor II (Sigma). For cyclohexamide (CHX) experiments, CHX (100μM) was added to striatal cells transfected with His-RasGRP1 and myc-Rhes constructs for an indicated time points and lysed for Western blotting. For immunoprecipitation experiments, protein lysates were pretreated with glutathione beads for one hour, glutathione beads were added, and the lysates were then rotated in a cold room for at least 5 hours. The beads were washed 3 times in binding buffer without a protease inhibitor cocktail, the proteins were eluted with 2X LDS-loading buffer and separated on 4-12% Bis-Tris Gel (Invitrogen), and then transferred to PVDF membranes and probed with the indicated antibodies. HRP-conjugated secondary antibodies (Jackson Immuno Research, Inc.) were probed to detect bound primary IgG with a chemiluminescence imager (Alpha Innotech) using enhanced chemiluminescence (ECL), from WesternBright Quantum (Advansta). For detecting protein interactions in the striatum, the freshly prepared striatal lysates (1 mg/ml protein) were pre-cleared with glutathione beads and incubated with of GST or GST-Rhes recombinant protein (1 μg) together with

glutathione beads (60 μl bead slurry) in binding buffer, overnight, and proceeded to Western blotting as before (8, 99).

In vitro binding

For the in vitro binding assays, an equimolar concentration of recombinant purified GST or GST-tagged Rhes wild-type or Rhes S33N was incubated with RasGRP1-FL for 16 hr at 4°C with glutathione beads in binding buffer containing 50 mM Tris/HCl (pH 8.2), 1 mM dithiothreitol, 100 mM NaCl, and 1% NP-40, and RasGRP1 was detected through Western blotting with a RasGRP1 antibody.

Recombinant protein purification

GST-RasGRP1-FL, GST-Rhes-wild-type, GST-Rhes-S33N, and Rhes D143N (all in pGEX-6P2) proteins were expressed as described earlier (8, 9, 18). Briefly, an *E. coli* BL21DE3 strain expressing pGEX-6P2 constructs was grown in 15 ml culture overnight and was transferred to 500 ml culture and grown until the log-phase was reached (−3.5 hr). The constructs were then treated with isopropyl β-D-1-thiogalactopyranoside (500 μM) for another 3 hr at 37°C. Cells were lysed by sonication in a lysis buffer containing 50 mM Tris/HCl (pH 8.2), 1 mM dithiothreitol, 100 mM NaCl, 2 mM EDTA, and 1% NP40, with protease inhibitor cocktails. The supernatant was exposed to GSH beads for 12 hr, and the beads were washed three times with a lysis buffer for 30 min. The recombinant proteins were eluted after treating the GST-bound beads with precision protease (10 units/overnight incubation in 50 mM Tris, 2 mM EDTA, and 1 mM DTT with 1% NP-40). The proteins were dialyzed against 50 mM HEPES, 2 mM EDTA, and 1 mM DTT, to remove detergent. For the GEF assay, the proteins were used immediately or were stored in aliquots at −80°C until further use.

GEF assay

A GEF assay was performed with 40 pmoles of Rhes (wild-type or mutant) or HRas and RasGRP1-FL, essentially as described before (100). Purified small GTPase samples were loaded with 2 mM GDP in a loading buffer (10 mM Hepes, pH 7.4, 100 mM Nacl, 2 mM EDTA, 0.2 mM DTT, 10 mM GDP) in 50μl total volume for 15 min, and were then stabilized with 1 mM $MgCl_2$ for 5 min. The exchange reaction was started with the addition of RasGRP1-FL in 50 μl of exchange buffer (10mM Hepes, pH 7.4, 100mM NaCl, 10mM MgCl2, 1mg/ml BSA, 0.2mM DTT, and 1mM GTP) and 10 μCi of GTP-γ-S^{35}. After 8 min, the reaction mixture was loaded onto the PROTRAN filter BA85 (Whatman) connected to a vacuum pump (Hoefer Scientific Instruments). The filter was washed with 1 ml of washing buffer (10 mM Hepes, pH 7.4, 100mM NaCl, and 5mM Mgcl2). The radioactivity was quantified on a phosphoimager (Bio-RAD, Molecular Imager).

Biochemical organelle separation and synaptosomal preparation

Striatal cells grown in 10cm plates (two or three) were pooled together and washed with cold PBS and treated in a homogenization buffer (0.25 M sucrose; 10 mM Tris, pH 7.4; 2 mM Mg-acetate; 0.5 mM EDTA; and protease inhibitor complex). The cells were homogenized using a 26g syringe by aspirating the cell suspension 12 times on ice. Cell lysates were then

loaded onto the top of a discontinuous sucrose gradient consisting of the following: 1 ml 0.25 M sucrose; 2 ml 0.5 M sucrose; 2 ml 0.8 M sucrose; 2.5 ml 1.16 M sucrose; 2.5 ml 1.3 M sucrose; and 1.5 ml 2 M sucrose. All sucrose density preparations were made in a gradient buffer (10 mM Tris, pH 7.4, and 1 mM Mg-acetate). The gradient was then centrifuged at 39,000 rpm for 2.5 h at 4°C in a Beckman SW41Ti rotor (Beckman Coulter, Brea, CA). Twelve fractions (1 ml each) were gently collected from the top. Equal volumes from each fraction were used for Western blot analysis. Synaptosome extraction was performed using the Syn-PER Reagent (Thermo Fisher Scientific) and nuclear/cytosolic fractionation was carried out using the kit from Biovision following the manufacturer's protocol.

Generation of Rhes and RasGRP1 single- and double-mutant mice

Rhes mutant mice(Rasd2^{tm1Rdl}) a targeted null/knockout used in our earlier studies (9, 11, 101) were obtained from Alessandro Usiello (20). We backcrossed *Rhes*$^{+/-}$ with C57BL/6 mice at least eight generations, and generated littermate wild-type controls and *Rhes*$^{-/-}$, which are fertile, phenotypically appear normal, and have normal motor learning behaviors, as tested on the rotating rod, consistent with previous reports (9, 11, 15, 18, 20, 101). B6.129P3-*Rasgrp1*^{tm1Jstn}/TbwnJ (102) mice were obtained from Jackson Laboratory (stock #022353) and are fertile, productive breeders; they have no gross abnormalities, which is consistent with previous reports (34, 102). Single- or double-mutant mice were obtained from harem breedings of double heterozygous *Rhes*$^{+/-}$/*Rasgrp1*$^{+/-}$ crossed with *Rhes*$^{+/-}$/*Rasgrp1*$^{+/-}$. This breeding scheme also resulted in several double/single het and homo combinations of mice (*Rhes*$^{+/-}$/*Rasgrp1*$^{+/-}$, *Rhes*$^{+/+}$/*Rasgrp1*$^{+/-}$, *Rhes*$^{+/-}$/*Rasgrp1*$^{+/+}$, *Rhes*$^{-/-}$/*Rasgrp1*$^{+/+}$, *Rhes*$^{+/+}$/*Rasgrp1*$^{-/-}$, *Rhes*$^{-/-}$/*Rasgrp1*$^{+/-}$, and *Rhes*$^{+/-}$/*Rasgrp1*$^{-/-}$). We adopted this commonly used breeding scheme to obtain single and double mutants and all the other respective groups. Mostly, we used heterozygous single- and double-mutant mice in this study to evaluate the potential dose-dependent and physiological effects of RasGRP1 and Rhes on basic or amphetamine-induced motor functions. We have adopted the above breeding strategy, as well as a backcrossing strategy of *Rhes*$^{-/-}$/*Rasgrp1*$^{+/-}$ x *Rhes*$^{-/-}$/*Rasgrp1*$^{+/-}$ and *Rhes*$^{-/+}$/*Rasgrp1*$^{-/-}$ x *Rhes*$^{-/+}$/*Rasgrp1*$^{-/-}$, and have obtained the required 6-8 double-mutant animals required for this study. All mice were cared for in accordance to the guidelines set forth by the National Institutes of Health regarding the proper treatment and use of laboratory animals and with approval of Institutional Animal Care and Use Committee of The Scripps Research Institute.

Behavioral Assay

Approximately three-month-old male and female mice were used for behavioral analysis in open-field activity chambers (40 × 40 × 40 cm) equipped with photocells (beam spacing 2.5cm) and locomotor activity and stereotypy counts were assessed on automated locomotor activity monitors using the VersaMax system software (Accuscan Instruments, Columbus, OH, USA). Mice were initially placed into the activity monitor chamber and allowed to habituate for 30 min, then were injected vehicle or with d-amphetamine (2 or 3mg/kg, i.p. at 10µl/g, dissolved in 0.9% saline), returned to the chamber, and monitored for 60 min after injection. Locomotor activity was measured in five minutes bins and reported as total

distance traveled over time. Stereotypy measures are also recorded by the system and reported herein.

Immunoprecipitation (IP) and Liquid chromatography-tandem mass spectrometry (LC-MS/MS)

Striatum was rapidly dissected out and homogenized in binding/lysis buffer (50 mM Tris, pH 7.4, 150 mM NaCl, 10% glycerol, 1.0% NP-40) with protease and phosphate inhibitors, followed by a brief sonication for 5 sec at 20% amplitude. Protein estimation was done using a BCA method and 1mg/ml concentration of protein lysates were pre-cleared with 50µl protein A/G beads for 1hr and the supernatant were incubated for 1hr at 4°C in Rhes IgG or control IgG then protein A/G beads were added and incubated overnight at 4°C. The number of mice used for each group per IP is provided in **Table S2**. The beads were washed five times with 1% NP-40 buffer (without protease/phosphatase inhibitor) and the protein samples were eluted with 30µl of 2X LDS containing + 1.5% β-mecaptoethanol. Protein samples were subjected to SDS-PAGE at 100 V for 18 min. The gel was Coomassie stained for 1 hour at room temperature with shaking, followed by destaining in water overnight. The gel bands were cut, in-gel treated with 10 mM DTT followed by 50 mM iodoacetamide, and subjected to trypsin digestion overnight. Prior to mass spectrometry analysis, the peptide pools were acidified, desalted through Zip-Tip C18 tip columns and dried down. Each sample was reconstructed in 100 µl of 0.1% formic acid 13µl were loaded into the system. Samples were analyzed by an Orbitrap Q Exactive or Orbitrap Fusion™ Tribrid™ Mass Spectrometer (Thermo Fisher Scientific), each one coupled to an EASY-nLC 1000 system. Peptides were concentrated and desalted on an RP pre-column (0.075 × 20 mm Acclaim PepMap 100 nano Viper, Thermo Fisher Scientific) and on-line eluted on an analytical RP column (0.075 × 250 mm Acclaim PepMap RLSC nano Viper, Thermo Fisher Scientific), operating at 300 nl/min using the following gradient: 5% B for 5 min, 5–40% B in 60 min, 40–80% B in 10 sec, 80% B for 5 min, 80-5% B in 10 sec, and 5% B for 20 min [solvent A: 0.1% formic acid (v/v); solvent B: 0.1% formic acid (v/v), 80% CH_3CN (v/v) (Thermo Fisher Scientific)]. The mass spectrometers were operated in a data-dependent MS/MS mode using the 10 most intense precursor ions detected in a survey scan from 380 to 1,400 *m/z* performed at 120K resolution. Tandem MS was performed by HCD fragmentation with normalized collision energy (NCE) of 27.0% for the Q Exactive and 30.0% for the Fusion. Protein identification was carried out using Mascot 2.3.01 (Matrix Science, UK) and Sequest algorithms (Proteome Discoverer v1.4, Thermo Scientific), allowing Oxidation (Met) as variable modifications. Other settings included Carbamidomethylation of Cys as fixed modification, three missed cleavages, and mass tolerance of 10 and 20 ppm for precursor and fragment ions, respectively. MS/MS raw files were searched against a mouse database along with human keratins, and porcine trypsin. The false discovery rates (FDR) of peptide identifications were calculated were calculated from the search results against a reverse sequences database; 1% FDR was used as criterion for peptide identification (the list of the peptide identification is presented in Data files S1-S4). The complete data set from the analysis of the “Rhesactome” (raw files, identification data and data analysis files) is available in the PeptideAtlas repository (http://www.peptideatlas.org/PASS/PASS00940) that can be downloaded via ftp://PASS00940:TF4767qx@ftp.peptideatlas.org/ .The PD search result files (.msf) were uploaded into Scaffold 4.3.2 (Proteome Software Inc., USA) for data

analysis and label-free quantitation. The biological replicates were combined as MudPIT, and the precursor ion intensities were used to quantitate peptide and protein identifications using a label free approach using Scaffold Q+ (version Scaffold_4.6.2, Proteome Software Inc., Portland, OR).

Statistical Analysis

Data are presented as mean ± SD or ± SEM as indicated. All experiments were performed at least in triplicate and repeated twice at minimum. Statistical analysis was performed using the Student's t-test, one-way analysis of variance (ANOVA) followed by Tukey's multiple comparison *post hoc* test or two-way repeated measures (mixed model) ANOVA followed by a *post hoc* Bonferroni multiple comparison test (Graph Pad Prism 6.0) as indicated in the figure legends.

Supplementary Material

Refer to Web version on PubMed Central for supplementary material.

ACKOWLEDGMENTS

We thank Melissa Benilous for administrative support. We thank Jill Crittenden and Ann M Graybiel of MIT for sharing the reagents. We like to thank Janet Hightower of Scripps-California for creating the model figures. We thank Lindsay Gorgen for the help in genotyping. **Funding:** This work was supported by grant from NIH/NINDS (R01-NS087019-01A1) to S. Subramaniam.

REFERENCES AND NOTES

1. Valjent E. Striatal signaling: two decades of progress. Front Neuroanat. 2012; 6:43. [PubMed: 23087620]
2. Beaulieu JM, Gainetdinov RR. The physiology, signaling, and pharmacology of dopamine receptors. Pharmacological reviews. 2011; 63:182–217. [PubMed: 21303898]
3. Di Chiara G, Morelli M, Consolo S. Modulatory functions of neurotransmitters in the striatum: ACh/dopamine/NMDA interactions. Trends in neurosciences. 1994; 17:228–233. [PubMed: 7521083]
4. Do J, Kim JI, Bakes J, Lee K, Kaang BK. Functional roles of neurotransmitters and neuromodulators in the dorsal striatum. Learning & memory. 2012; 20:21–28. [PubMed: 23247251]
5. Cenci MA, Konradi C. Maladaptive striatal plasticity in L-DOPA-induced dyskinesia. Progress in brain research. 2010; 183:209–233. [PubMed: 20696322]
6. Paleacu D. Tetrabenazine in the treatment of Huntington's disease. Neuropsychiatric disease and treatment. 2007; 3:545–551. [PubMed: 19381278]
7. Falk JD, Vargiu P, Foye PE, Usui H, Perez J, Danielson PE, Lerner DL, Bernal J, Sutcliffe JG. Rhes: A striatal-specific Ras homolog related to Dexras1. J Neurosci Res. 1999; 57:782–788. [PubMed: 10467249]
8. Subramaniam S, Sixt KM, Barrow R, Snyder SH. Rhes, a striatal specific protein, mediates mutant-huntingtin cytotoxicity. Science. 2009; 324:1327–1330. [PubMed: 19498170]
9. Subramaniam S, Mealer RG, Sixt KM, Barrow RK, Usiello A, Snyder SH. Rhes, a physiologic regulator of sumoylation, enhances cross-sumoylation between the basic sumoylation enzymes E1 and Ubc9. The Journal of biological chemistry. 2010; 285:20428–20432. [PubMed: 20424159]
10. Mealer RG, Murray AJ, Shahani N, Subramaniam S, Snyder SH. Rhes, a Striatal-Selective Protein Implicated in Huntington Disease, Binds Beclin-1 and Activates Autophagy. The Journal of biological chemistry. 2013

11. Swarnkar S, Chen Y, Pryor WM, Shahani N, Page DT, Subramaniam S. Ectopic expression of the striatal-enriched GTPase Rhes elicits cerebellar degeneration and an ataxia phenotype in Huntington's disease. Neurobiology of disease. 2015; 82:66–77. [PubMed: 26048156]
12. Okamoto S, Pouladi MA, Talantova M, Yao D, Xia P, Ehrnhoefer DE, Zaidi R, Clemente A, Kaul M, Graham RK, Zhang D, Vincent Chen HS, Tong G, Hayden MR, Lipton SA. Balance between synaptic versus extrasynaptic NMDA receptor activity influences inclusions and neurotoxicity of mutant huntingtin. Nat Med. 2009; 15:1407–1413. [PubMed: 19915593]
13. Seredenina T, Gokce O, Luthi-Carter R. Decreased striatal RGS2 expression is neuroprotective in Huntington's disease (HD) and exemplifies a compensatory aspect of HD-induced gene regulation. PloS one. 2011; 6:e22231. [PubMed: 21779398]
14. Lu B, Palacino J. A novel human embryonic stem cell-derived Huntington's disease neuronal model exhibits mutant huntingtin (mHTT) aggregates and soluble mHTT-dependent neurodegeneration. FASEB J. 2013
15. Baiamonte BA, Lee FA, Brewer ST, Spano D, LaHoste GJ. Attenuation of Rhes activity significantly delays the appearance of behavioral symptoms in a mouse model of Huntington's disease. PloS one. 2013; 8:e53606. [PubMed: 23349722]
16. Sbodio JI, Paul BD, Machamer CE, Snyder SH. Golgi protein ACBD3 mediates neurotoxicity associated with Huntington's disease. Cell Rep. 2013; 4:890–897. [PubMed: 24012756]
17. Argenti, M. Ph.D Thesis, Università degli Studi di Padova. Padova PD, Italy: 2014. THE ROLE OF MITOCHONDRIAL DYSFUNCTION IN HUNTINGTON'S DISEASE PATHOGENESIS AND ITS RELATION WITH STRIATAL RHES PROTEIN..
18. Subramaniam S, Napolitano F, Mealer RG, Kim S, Errico F, Barrow R, Shahani N, Tyagi R, Snyder SH, Usiello A. Rhes, a striatal-enriched small G protein, mediates mTOR signaling and L-DOPA-induced dyskinesia. Nature neuroscience. 2012; 15:191–193.
19. Brugnoli A, Napolitano F, Usiello A, Morari M. Genetic deletion of Rhes or pharmacological blockade of mTORC1 prevent striato-nigral neurons activation in levodopa-induced dyskinesia. Neurobiology of disease. 2015
20. Errico F, Santini E, Migliarini S, Borgkvist A, Centonze D, Nasti V, Carta M, De Chiara V, Prosperetti C, Spano D, Herve D, Pasqualetti M, Di Lauro R, Fisone G, Usiello A. The GTP-binding protein Rhes modulates dopamine signalling in striatal medium spiny neurons. Molecular and cellular neurosciences. 2008; 37:335–345. [PubMed: 18035555]
21. Quintero GC, Spano D. Exploration of sex differences in Rhes effects in dopamine mediated behaviors. Neuropsychiatric disease and treatment. 2011; 7:697–706. [PubMed: 22128255]
22. Quintero GC, Spano D, Lahoste GJ, Harrison LM. The Ras homolog Rhes affects dopamine D1 and D2 receptor-mediated behavior in mice. Neuroreport. 2008; 19:1563–1566. [PubMed: 18845937]
23. Lee FA, Baiamonte BA, Spano D, Lahoste GJ, Soignier RD, Harrison LM. Mice lacking rhes show altered morphine analgesia, tolerance, and dependence. Neurosci Lett. 2011; 489:182–186. [PubMed: 21163334]
24. Vitucci D, Di Giorgio A, Napolitano F, Pelosi B, Blasi G, Errico F, Attrotto MT, Gelao B, Fazio L, Taurisano P, Di Maio A, Marsili V, Pasqualetti M, Bertolino A, Usiello A. Rasd2 Modulates Prefronto-Striatal Phenotypes in Humans and 'Schizophrenia-Like Behaviors' in Mice. Neuropsychopharmacology : official publication of the American College of Neuropsychopharmacology. 2015
25. Ebinu JO, Bottorff DA, Chan EY, Stang SL, Dunn RJ, Stone JC. RasGRP, a Ras guanyl nucleotide-releasing protein with calcium- and diacylglycerol-binding motifs. Science. 1998; 280:1082–1086. [PubMed: 9582122]
26. Tognon CE, Kirk HE, Passmore LA, Whitehead IP, Der CJ, Kay RJ. Regulation of RasGRP via a phorbol ester-responsive C1 domain. Mol Cell Biol. 1998; 18:6995–7008. [PubMed: 9819387]
27. Kawasaki H, Springett GM, Toki S, Canales JJ, Harlan P, Blumenstiel JP, Chen EJ, Bany IA, Mochizuki N, Ashbacher A, Matsuda M, Housman DE, Graybiel AM. A Rap guanine nucleotide exchange factor enriched highly in the basal ganglia. Proceedings of the National Academy of Sciences of the United States of America. 1998; 95:13278–13283. [PubMed: 9789079]

28. Crittenden JR, Cantuti-Castelvetri I, Saka E, Keller-McGandy CE, Hernandez LF, Kett LR, Young AB, Standaert DG, Graybiel AM. Dysregulation of CalDAG-GEFI and CalDAG-GEFII predicts the severity of motor side-effects induced by anti-parkinsonian therapy. Proceedings of the National Academy of Sciences of the United States of America. 2009; 106:2892–2896. [PubMed: 19171906]
29. Coughlin JJ, Stang SL, Dower NA, Stone JC. RasGRP1 and RasGRP3 regulate B cell proliferation by facilitating B cell receptor-Ras signaling. J Immunol. 2005; 175:7179–7184. [PubMed: 16301621]
30. Bartlett A, Buhlmann JE, Stone J, Lim B, Barrington RA. Multiple checkpoint breach of B cell tolerance in Rasgrp1-deficient mice. J Immunol. 2013; 191:3605–3613. [PubMed: 23997211]
31. Iwig JS, Vercoulen Y, Das R, Barros T, Limnander A, Che Y, Pelton JG, Wemmer DE, Roose JP, Kuriyan J. Structural analysis of autoinhibition in the Ras-specific exchange factor RasGRP1. eLife. 2013; 2:e00813. [PubMed: 23908768]
32. Hartzell C, Ksionda O, Lemmens E, Coakley K, Yang M, Dail M, Harvey RC, Govern C, Bakker J, Lenstra TL, Ammon K, Boeter A, Winter SS, Loh M, Shannon K, Chakraborty AK, Wabl M, Roose JP. Dysregulated RasGRP1 responds to cytokine receptor input in T cell leukemogenesis. Sci Signal. 2013; 6:ra21. [PubMed: 23532335]
33. Rapoport MJ, Bloch O, Amit-Vasina M, Yona E, Molad Y. Constitutive abnormal expression of RasGRP-1 isoforms and low expression of PARP-1 in patients with systemic lupus erythematosus. Lupus. 2011; 20:1501–1509. [PubMed: 21976405]
34. Spano D, Branchi I, Rosica A, Pirro MT, Riccio A, Mithbaokar P, Affuso A, Arra C, Campolongo P, Terracciano D, Macchia V, Bernal J, Alleva E, Di Lauro R. Rhes is involved in striatal function. Mol Cell Biol. 2004; 24:5788–5796. [PubMed: 15199135]
35. Harrison LM, Muller SH, Spano D. Effects of the Ras homolog Rhes on Akt/protein kinase B and glycogen synthase kinase 3 phosphorylation in striatum. Neuroscience. 2013; 236:21–30. [PubMed: 23380502]
36. Vargiu P, De Abajo R, Garcia-Ranea JA, Valencia A, Santisteban P, Crespo P, Bernal J. The small GTP-binding protein, Rhes, regulates signal transduction from G protein-coupled receptors. Oncogene. 2004; 23:559–568. [PubMed: 14724584]
37. Bardo MT. Neuropharmacological mechanisms of drug reward: beyond dopamine in the nucleus accumbens. Crit Rev Neurobiol. 1998; 12:37–67. [PubMed: 9444481]
38. Ungerstedt U. Striatal dopamine release after amphetamine or nerve degeneration revealed by rotational behaviour. Acta physiologica Scandinavica. Supplementum. 1971; 367:49–68.
39. Laruelle M, Abi-Dargham A, van Dyck CH, Rosenblatt W, Zea-Ponce Y, Zoghbi SS, Baldwin RM, Charney DS, Hoffer PB, Kung HF, et al. SPECT imaging of striatal dopamine release after amphetamine challenge. J Nucl Med. 1995; 36:1182–1190. [PubMed: 7790942]
40. Meyer AC, Bardo MT. Amphetamine self-administration and dopamine function: assessment of gene × environment interactions in Lewis and Fischer 344 rats. Psychopharmacology (Berl). 2015; 232:2275–2285. [PubMed: 25566972]
41. Weiss VG, Hofford RS, Yates JR, Jennings FC, Bardo MT. Sex differences in monoamines following amphetamine and social reward in adolescent rats. Exp Clin Psychopharmacol. 2015; 23:197–205. [PubMed: 26237317]
42. Kelley AE. Measurement of rodent stereotyped behavior. Curr Protoc Neurosci. 2001 Chapter 8, Unit 8 8.
43. North RB, Harik SI, Snyder SH. Amphetamine isomers: influences on locomotor and stereotyped behavior of cats. Pharmacol Biochem Behav. 1974; 2:115–118. [PubMed: 4857222]
44. Yates JW, Meij JT, Sullivan JR, Richtand NM, Yu L. Bimodal effect of amphetamine on motor behaviors in C57BL/6 mice. Neurosci Lett. 2007; 427:66–70. [PubMed: 17920769]
45. Graybiel AM, Grafton ST. The striatum: where skills and habits meet. Cold Spring Harbor perspectives in biology. 2015; 7:a021691. [PubMed: 26238359]
46. Ikeda H, Adachi K, Fujita S, Tomiyama K, Saigusa T, Kobayashi M, Koshikawa N, Waddington JL. Investigating complex basal ganglia circuitry in the regulation of motor behaviour, with particular focus on orofacial movement. Behavioural pharmacology. 2015; 26:18–32. [PubMed: 25485640]

47. Kravitz AV, Kreitzer AC. Striatal mechanisms underlying movement, reinforcement, and punishment. Physiology. 2012; 27:167–177. [PubMed: 22689792]
48. Besson MJ, Cheramy A, Feltz P, Glowinski J. Release of newly synthesized dopamine from dopamine-containing terminals in the striatum of the rat. Proceedings of the National Academy of Sciences of the United States of America. 1969; 62:741–748. [PubMed: 4389748]
49. Fleckenstein AE, Volz TJ, Riddle EL, Gibb JW, Hanson GR. New insights into the mechanism of action of amphetamines. Annual review of pharmacology and toxicology. 2007; 47:681–698.
50. Harrison LM. Rhes: a GTP-binding protein integral to striatal physiology and pathology. Cell Mol Neurobiol. 2012; 32:907–918. [PubMed: 22450871]
51. Ghiglieri V, Napolitano F, Pelosi B, Schepisi C, Migliarini S, Di Maio A, Pendolino V, Mancini M, Sciamanna G, Vitucci D, Maddaloni G, Giampa C, Errico F, Nistico R, Pasqualetti M, Picconi B, Usiello A. Rhes influences striatal cAMP/PKA-dependent signaling and synaptic plasticity in a gender-sensitive fashion. Scientific reports. 2015; 5:10933. [PubMed: 26190541]
52. Han K, Holder JL Jr. Schaaf CP, Lu H, Chen H, Kang H, Tang J, Wu Z, Hao S, Cheung SW, Yu P, Sun H, Breman AM, Patel A, Lu HC, Zoghbi HY. SHANK3 overexpression causes manic-like behaviour with unique pharmacogenetic properties. Nature. 2013; 503:72–77. [PubMed: 24153177]
53. Ventura R, Pascucci T, Catania MV, Musumeci SA, Puglisi-Allegra S. Object recognition impairment in Fmr1 knockout mice is reversed by amphetamine: involvement of dopamine in the medial prefrontal cortex. Behavioural pharmacology. 2004; 15:433–442. [PubMed: 15343070]
54. Ehrman LA, Williams MT, Schaefer TL, Gudelsky GA, Reed TM, Fienberg AA, Greengard P, Vorhees CV. Phosphodiesterase 1B differentially modulates the effects of methamphetamine on locomotor activity and spatial learning through DARPP32-dependent pathways: evidence from PDE1B-DARPP32 double-knockout mice. Genes, brain, and behavior. 2006; 5:540–551.
55. Beaulieu JM, Sotnikova TD, Yao WD, Kockeritz L, Woodgett JR, Gainetdinov RR, Caron MG. Lithium antagonizes dopamine-dependent behaviors mediated by an AKT/glycogen synthase kinase 3 signaling cascade. Proceedings of the National Academy of Sciences of the United States of America. 2004; 101:5099–5104. [PubMed: 15044694]
56. Beaulieu JM, Sotnikova TD, Marion S, Lefkowitz RJ, Gainetdinov RR, Caron MG. An Akt/beta-arrestin 2/PP2A signaling complex mediates dopaminergic neurotransmission and behavior. Cell. 2005; 122:261–273. [PubMed: 16051150]
57. Bang S, Steenstra C, Kim SF. Striatum specific protein, Rhes regulates AKT pathway. Neurosci Lett. 2012; 521:142–147. [PubMed: 22683505]
58. McPherson PS, Kay BK, Hussain NK. Signaling on the endocytic pathway. Traffic. 2001; 2:375–384. [PubMed: 11389765]
59. Rappoport JZ. Focusing on clathrin-mediated endocytosis. The Biochemical journal. 2008; 412:415–423. [PubMed: 18498251]
60. Bohdanowicz M, Grinstein S. Role of phospholipids in endocytosis, phagocytosis, and macropinocytosis. Physiological reviews. 2013; 93:69–106. [PubMed: 23303906]
61. Ciobanu DC, Lu L, Mozhui K, Wang X, Jagalur M, Morris JA, Taylor WL, Dietz K, Simon P, Williams RW. Detection, validation, and downstream analysis of allelic variation in gene expression. Genetics. 2010; 184:119–128. [PubMed: 19884314]
62. Geiss-Friedlander R, Melchior F. Concepts in sumoylation: a decade on. Nature reviews. Molecular cell biology. 2007; 8:947–956. [PubMed: 18000527]
63. Aron AR, Schlaghecken F, Fletcher PC, Bullmore ET, Eimer M, Barker R, Sahakian BJ, Robbins TW. Inhibition of subliminally primed responses is mediated by the caudate and thalamus: evidence from functional MRI and Huntington's disease. Brain : a journal of neurology. 2003; 126:713–723. [PubMed: 12566291]
64. Deveney CM, Connolly ME, Jenkins SE, Kim P, Fromm SJ, Brotman MA, Pine DS, Leibenluft E. Striatal dysfunction during failed motor inhibition in children at risk for bipolar disorder. Progress in neuro-psychopharmacology & biological psychiatry. 2012; 38:127–133. [PubMed: 22414616]
65. Diamond A. Attention-deficit disorder (attention-deficit/ hyperactivity disorder without hyperactivity): a neurobiologically and behaviorally distinct disorder from attention-deficit/

hyperactivity disorder (with hyperactivity). Development and psychopathology. 2005; 17:807–825. [PubMed: 16262993]

66. Gauggel S, Rieger M, Feghoff TA. Inhibition of ongoing responses in patients with Parkinson's disease. Journal of neurology, neurosurgery, and psychiatry. 2004; 75:539–544.
67. Morein-Zamir S, Robbins TW. Fronto-striatal circuits in response-inhibition: Relevance to addiction. Brain research. 2015; 1628:117–129. [PubMed: 25218611]
68. Winterer G, Weinberger DR. Genes, dopamine and cortical signal-to-noise ratio in schizophrenia. Trends in neurosciences. 2004; 27:683–690. [PubMed: 15474169]
69. Liu YL, Fann CS, Liu CM, Chen WJ, Wu JY, Hung SI, Chen CH, Jou YS, Liu SK, Hwang TJ, Hsieh MH, Chang CC, Yang WC, Lin JJ, Chou FH, Faraone SV, Tsuang MT, Hwu HG. RASD2, MYH9, and CACNG2 genes at chromosome 22q12 associated with the subgroup of schizophrenia with non-deficit in sustained attention and executive function. Biological psychiatry. 2008; 64:789–796. [PubMed: 18571626]
70. Yang HC, Liu CM, Liu YL, Chen CW, Chang CC, Fann CS, Chiou JJ, Yang UC, Chen CH, Faraone SV, Tsuang MT, Hwu HG. The DAO gene is associated with schizophrenia and interacts with other genes in the Taiwan Han Chinese population. PloS one. 2013; 8:e60099. [PubMed: 23555897]
71. Ferreira MA, O'Donovan MC, Meng YA, Jones IR, Ruderfer DM, Jones L, Fan J, Kirov G, Perlis RH, Green EK, Smoller JW, Grozeva D, Stone J, Nikolov I, Chambert K, Hamshere ML, Nimgaonkar VL, Moskvina V, Thase ME, Caesar S, Sachs GS, Franklin J, Gordon-Smith K, Ardlie KG, Gabriel SB, Fraser C, Blumenstiel B, Defelice M, Breen G, Gill M, Morris DW, Elkin A, Muir WJ, McGhee KA, Williamson R, MacIntyre DJ, MacLean AW, St CD, Robinson M, Van Beck M, Pereira AC, Kandaswamy R, McQuillin A, Collier DA, Bass NJ, Young AH, Lawrence J, Ferrier IN, Anjorin A, Farmer A, Curtis D, Scolnick EM, McGuffin P, Daly MJ, Corvin AP, Holmans PA, Blackwood DH, Gurling HM, Owen MJ, Purcell SM, Sklar P, Craddock N, C. Wellcome Trust Case Control. Collaborative genome-wide association analysis supports a role for ANK3 and CACNA1C in bipolar disorder. Nature genetics. 2008; 40:1056–1058. [PubMed: 18711365]
72. Francardo V, Cenci MA. Investigating the molecular mechanisms of L-DOPA-induced dyskinesia in the mouse. Parkinsonism & related disorders. 2014; 20(Suppl 1):S20–22. [PubMed: 24262181]
73. Arnold LE, Wender PH, McCloskey K, Snyder SH. Levoamphetamine and dextroamphetamine: comparative efficacy in the hyperkinetic syndrome. Assessment by target symptoms. Archives of general psychiatry. 1972; 27:816–822. [PubMed: 4564954]
74. Rawson RA, Condon TP. Why do we need an Addiction supplement focused on methamphetamine? Addiction. 2007; 102(Suppl 1):1–4.
75. Berman S, O'Neill J, Fears S, Bartzokis G, London ED. Abuse of amphetamines and structural abnormalities in the brain. Ann N Y Acad Sci. 2008; 1141:195–220. [PubMed: 18991959]
76. Sulzer D. How addictive drugs disrupt presynaptic dopamine neurotransmission. Neuron. 2011; 69:628–649. [PubMed: 21338876]
77. Peterson SM, Pack TF, Wilkins AD, Urs NM, Urban DJ, Bass CE, Lichtarge O, Caron MG. Elucidation of G-protein and beta-arrestin functional selectivity at the dopamine D2 receptor. Proceedings of the National Academy of Sciences of the United States of America. 2015; 112:7097–7102. [PubMed: 25964346]
78. London ED, Simon SL, Berman SM, Mandelkern MA, Lichtman AM, Bramen J, Shinn AK, Miotto K, Learn J, Dong Y, Matochik JA, Kurian V, Newton T, Woods R, Rawson R, Ling W. Mood disturbances and regional cerebral metabolic abnormalities in recently abstinent methamphetamine abusers. Archives of general psychiatry. 2004; 61:73–84. [PubMed: 14706946]
79. Hart AB, Gamazon ER, Engelhardt BE, Sklar P, Kahler AK, Hultman CM, Sullivan PF, Neale BM, Faraone SV, de Wit H, Cox NJ, Palmer AA. Genetic variation associated with euphorigenic effects of d-amphetamine is associated with diminished risk for schizophrenia and attention deficit hyperactivity disorder. Proceedings of the National Academy of Sciences of the United States of America. 2014; 111:5968–5973. [PubMed: 24711425]
80. Graybiel AM, Moratalla R, Robertson HA. Amphetamine and cocaine induce drug-specific activation of the c-fos gene in striosome-matrix compartments and limbic subdivisions of the

striatum. Proceedings of the National Academy of Sciences of the United States of America. 1990; 87:6912–6916. [PubMed: 2118661]

81. Konradi C, Cole RL, Heckers S, Hyman SE. Amphetamine regulates gene expression in rat striatum via transcription factor CREB. The Journal of neuroscience : the official journal of the Society for Neuroscience. 1994; 14:5623–5634. [PubMed: 8083758]
82. McGinty JF, Bache AJ, Coleman NT, Sun WL. The Role of BDNF/TrkB Signaling in Acute Amphetamine-Induced Locomotor Activity and Opioid Peptide Gene Expression in the Rat Dorsal Striatum. Frontiers in systems neuroscience. 2011; 5:60. [PubMed: 21811445]
83. Wang JQ, Daunais JB, McGinty JF. NMDA receptors mediate amphetamine-induced upregulation of zif/268 and preprodynorphin mRNA expression in rat striatum. Synapse. 1994; 18:343–353. [PubMed: 7886627]
84. Chen JF, Beilstein M, Xu YH, Turner TJ, Moratalla R, Standaert DG, Aloyo VJ, Fink JS, Schwarzschild MA. Selective attenuation of psychostimulant-induced behavioral responses in mice lacking A(2A) adenosine receptors. Neuroscience. 2000; 97:195–204. [PubMed: 10771351]
85. Brandon EP, Logue SF, Adams MR, Qi M, Sullivan SP, Matsumoto AM, Dorsa DM, Wehner JM, McKnight GS, Idzerda RL. Defective motor behavior and neural gene expression in RIIbeta-protein kinase A mutant mice. The Journal of neuroscience : the official journal of the Society for Neuroscience. 1998; 18:3639–3649. [PubMed: 9570795]
86. Steinkellner T, Mus L, Eisenrauch B, Constantinescu A, Leo D, Konrad L, Rickhag M, Sorensen G, Efimova EV, Kong E, Willeit M, Sotnikova TD, Kudlacek O, Gether U, Freissmuth M, Pollak DD, Gainetdinov RR, Sitte HH. In vivo amphetamine action is contingent on alphaCaMKII. Neuropsychopharmacology : official publication of the American College of Neuropsychopharmacology. 2014; 39:2681–2693. [PubMed: 24871545]
87. Salahpour A, Ramsey AJ, Medvedev IO, Kile B, Sotnikova TD, Holmstrand E, Ghisi V, Nicholls PJ, Wong L, Murphy K, Sesack SR, Wightman RM, Gainetdinov RR, Caron MG. Increased amphetamine-induced hyperactivity and reward in mice overexpressing the dopamine transporter. Proceedings of the National Academy of Sciences of the United States of America. 2008; 105:4405–4410. [PubMed: 18347339]
88. Buller AL, Larson HC, Schneider BE, Beaton JA, Morrisett RA, Monaghan DT. The molecular basis of NMDA receptor subtypes: native receptor diversity is predicted by subunit composition. The Journal of neuroscience : the official journal of the Society for Neuroscience. 1994; 14:5471–5484. [PubMed: 7916045]
89. Gangarossa G, Longueville S, De Bundel D, Perroy J, Herve D, Girault JA, Valjent E. Characterization of dopamine D1 and D2 receptor-expressing neurons in the mouse hippocampus. Hippocampus. 2012; 22:2199–2207. [PubMed: 22777829]
90. Nairn AC, Hemmings HC Jr. Greengard P. Protein kinases in the brain. Annual review of biochemistry. 1985; 54:931–976.
91. Leroy K, Brion JP. Developmental expression and localization of glycogen synthase kinase-3beta in rat brain. Journal of chemical neuroanatomy. 1999; 16:279–293. [PubMed: 10450875]
92. Hill C, Goddard A, Ladds G, Davey J. The cationic region of Rhes mediates its interactions with specific Gbeta subunits. Cell Physiol Biochem. 2009; 23:1–8. [PubMed: 19255495]
93. Huttlin EL, Ting L, Bruckner RJ, Gebreab F, Gygi MP, Szpyt J, Tam S, Zarraga G, Colby G, Baltier K, Dong R, Guarani V, Vaites LP, Ordureau A, Rad R, Erickson BK, Wuhr M, Chick J, Zhai B, Kolippakkam D, Mintseris J, Obar RA, Harris T, Artavanis-Tsakonas S, Sowa ME, De Camilli P, Paulo JA, Harper JW, Gygi SP. The BioPlex Network: A Systematic Exploration of the Human Interactome. Cell. 2015; 162:425–440. [PubMed: 26186194]
94. Venkatesan K, Rual JF, Vazquez A, Stelzl U, Lemmens I, Hirozane-Kishikawa T, Hao T, Zenkner M, Xin X, Goh KI, Yildirim MA, Simonis N, Heinzmann K, Gebreab F, Sahalie JM, Cevik S, Simon C, de Smet AS, Dann E, Smolyar A, Vinayagam A, Yu H, Szeto D, Borick H, Dricot A, Klitgord N, Murray RR, Lin C, Lalowski M, Timm J, Rau K, Boone C, Braun P, Cusick ME, Roth FP, Hill DE, Tavernier J, Wanker EE, Barabasi AL, Vidal M. An empirical framework for binary interactome mapping. Nature methods. 2009; 6:83–90. [PubMed: 19060904]
95. Havugimana PC, Hart GT, Nepusz T, Yang H, Turinsky AL, Li Z, Wang PI, Boutz DR, Fong V, Phanse S, Babu M, Craig SA, Hu P, Wan C, Vlasblom J, Dar VU, Bezginov A, Clark GW, Wu GC,

Wodak SJ, Tillier ER, Paccanaro A, Marcotte EM, Emili A. A census of human soluble protein complexes. Cell. 2012; 150:1068–1081. [PubMed: 22939629]

96. Topham MK, Prescott SM. Diacylglycerol kinase zeta regulates Ras activation by a novel mechanism. The Journal of cell biology. 2001; 152:1135–1143. [PubMed: 11257115]
97. Ewing RM, Chu P, Elisma F, Li H, Taylor P, Climie S, McBroom-Cerajewski L, Robinson MD, O'Connor L, Li M, Taylor R, Dharsee M, Ho Y, Heilbut A, Moore L, Zhang S, Ornatsky O, Bukhman YV, Ethier M, Sheng Y, Vasilescu J, Abu-Farha M, Lambert JP, Duewel HS, Stewart II, Kuehl B, Hogue K, Colwill K, Gladwish K, Muskat B, Kinach R, Adams SL, Moran MF, Morin GB, Topaloglou T, Figeys D. Large-scale mapping of human protein-protein interactions by mass spectrometry. Molecular systems biology. 2007; 3:89. [PubMed: 17353931]
98. Shahani N, Pryor W, Swarnkar S, Kholodilov N, Thinakaran G, Burke RE, Subramaniam S. Rheb GTPase regulates beta-secretase levels and amyloid beta generation. The Journal of biological chemistry. 2014; 289:5799–5808. [PubMed: 24368770]
99. Pryor WM, Biagioli M, Shahani N, Swarnkar S, Huang WC, Page DT, MacDonald ME, Subramaniam S. Huntingtin promotes mTORC1 signaling in the pathogenesis of Huntington's disease. Sci Signal. 2014; 7:ra103. [PubMed: 25351248]
100. Vouri, J.-F. C. a. K. Regulators and Effectors of Small GTPases: Rho Family: Rho Family. Vol. 406. Elsevier Academic Press; U.S.A: 2006. In vitro Guanine-nucleotide Exchange activity of DHR-2/DOCKER/CZH2 domains.
101. Mealer RG, Subramaniam S, Snyder SH. Rhes deletion is neuroprotective in the 3-nitropropionic acid model of Huntington's disease. The Journal of neuroscience : the official journal of the Society for Neuroscience. 2013; 33:4206–4210. [PubMed: 23447628]
102. Dower NA, Stang SL, Bottorff DA, Ebinu JO, Dickie P, Ostergaard HL, Stone JC. RasGRP is essential for mouse thymocyte differentiation and TCR signaling. Nat Immunol. 2000; 1:317–321. [PubMed: 11017103]

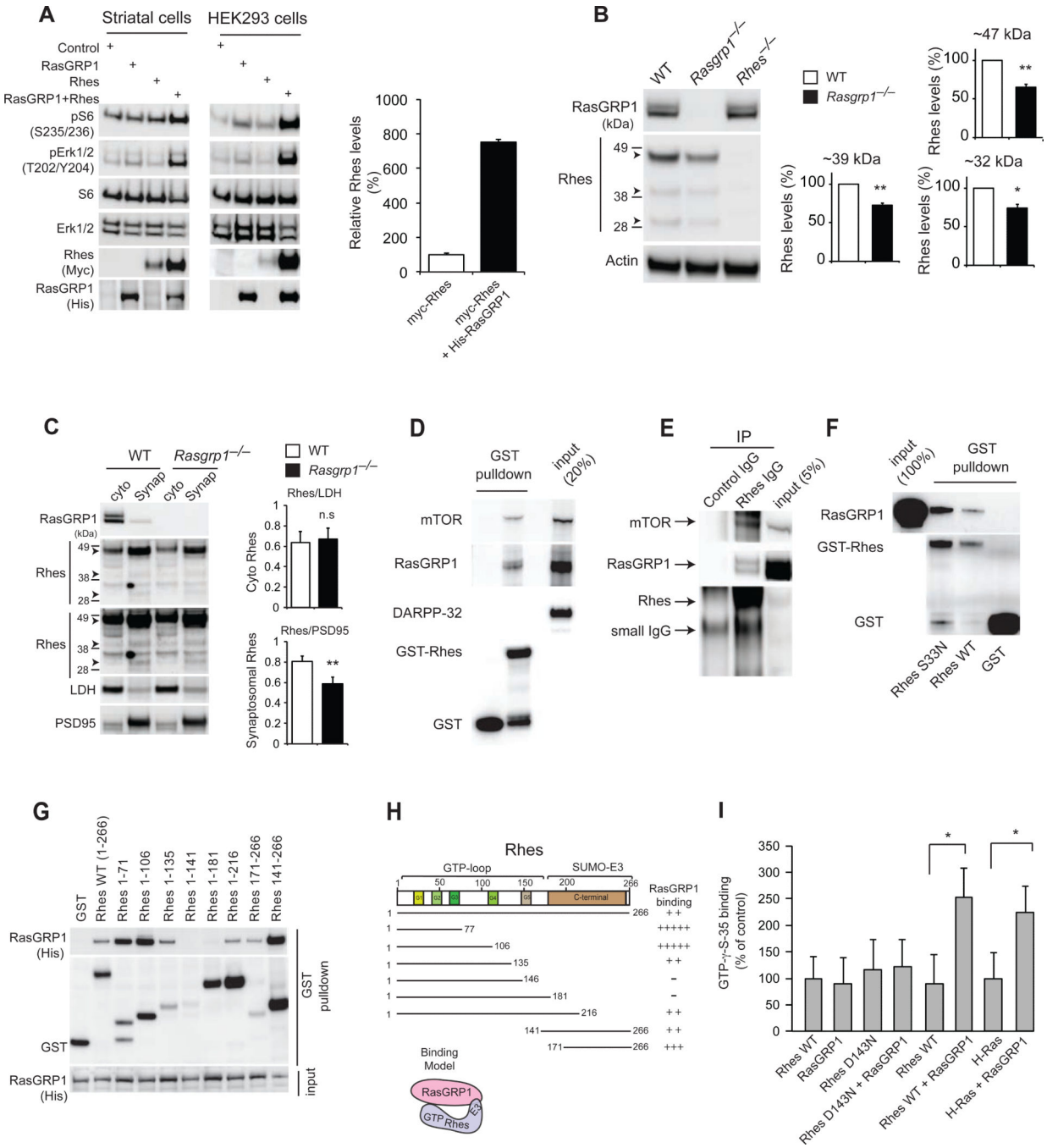

Figure 1. RasGRP1 interacts with Rhes in the striatum

(A) Western blot analysis of the abundance of myc-tagged Rhes, phosphorylated and total S6, ERK, and other indicated proteins in cultured striatal neuronal cells (*STHdh*$^{Q7/Q7}$) and HEK293 cells transfected with His-tagged RasGRP1. Right, quantification of Rhes in striatal cells. **(B)**. Western blot analysis of Rhes (47kD, 39kD, and 32kD, arrowheads) in striatal lysates from wild-type and *Rasgrp1*$^{-/-}$ mice. (**C**). Cytoplasmic (cyto) and synaptosomal (synap) separation of Rhes from the striatum of wild-type and *Rasgrp1*$^{-/-}$ mice. Cytosolic (LDH) and synaptosomal (PSD-95) markers are indicated. **(D)** Western blot

analysis of GST-Rhes interaction with endogenous RasGRP1, mTOR or DARPP-32 in the striatal lysates. **(E)** Immunoprecipitation (IP) of Rhes with Rhes IgG or control IgG and Western blotting for endogenous mTOR or RasGRP1. **(F)** Western blotting to assess the interaction of purified RasGRP1 with wild-type or S33N mutant GST-Rhes in vitro. **(G)** Domain interaction of GST-Rhes wild-type or various Rhes fragments with overexpressed His-RasGRP1 in HEK293 cells. **(H)** Interaction model showing two-point interaction (N-terminal and C-terminal E3 ligase domain) of Rhes with RasGRP1. **(I)** Radiolabelling filter-binding GEF assay was performed using recombinant RasGRP1 and Rhes (wild-type, D143N) or H-Ras proteins. The amount of GTPγS-35 bound on membrane was imaged and signals were quantified. Data are means ± SEM, n=3-5 experiments. *$p<0.05$ and **$p<0.01$ by a Student's *t*-test.

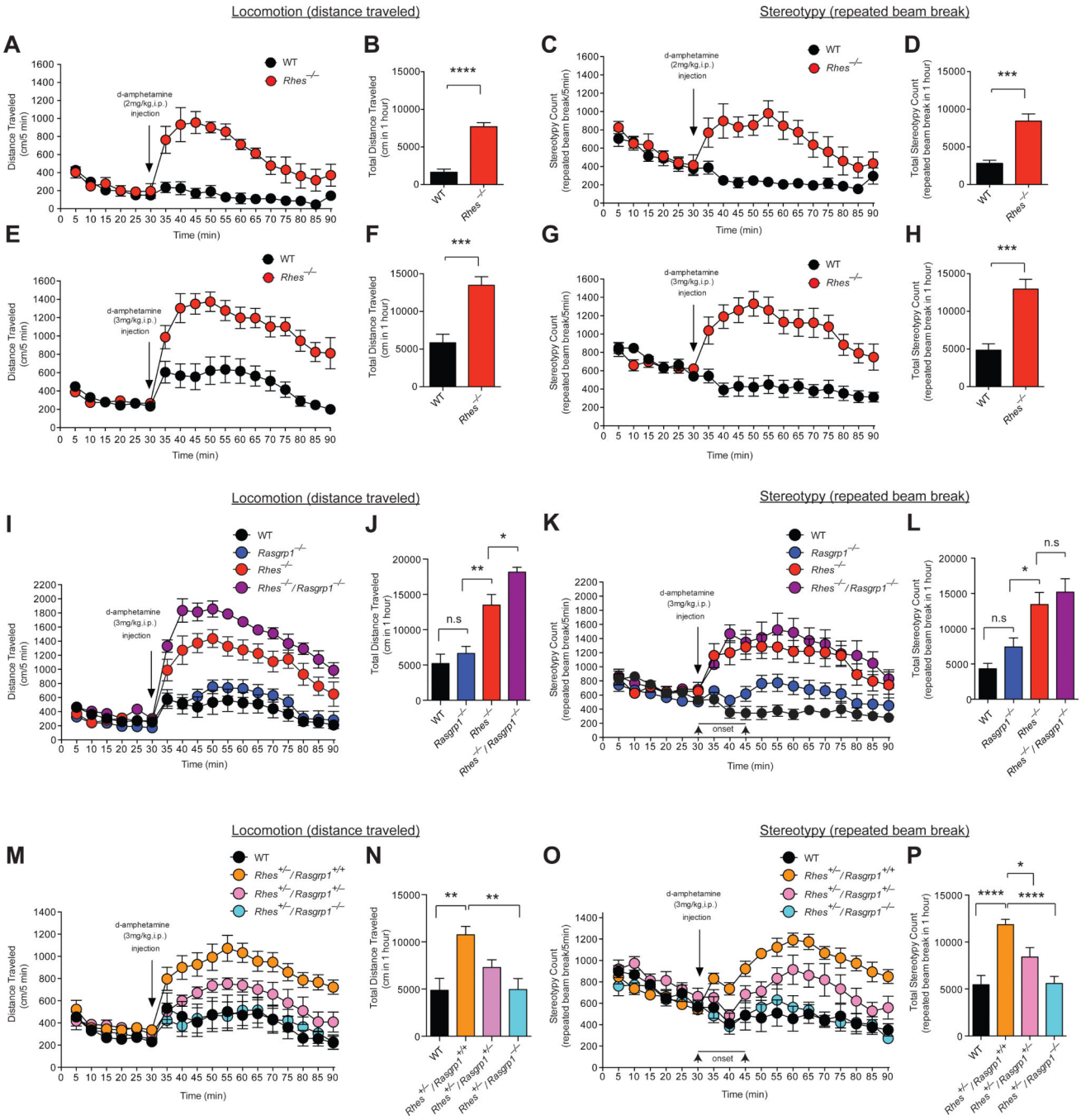

Figure 2. RasGRP1 inhibits Rhes to promote motor behavior

(A-D) Motor behaviors in wild-type and *Rhes*$^{-/-}$ mice upon injection of 2mg/kg d-amphetamine (i.p. at 10μl/g). n=6 wild-type (2 female), n=4 *Rhes*$^{-/-}$ mice (2 female). **(A)** Distance (cm) traveled per 5 min. F value for genotype: $F_{(1,8)}$=56.27, p<0.0001; for time: $F_{(17,136)}$=9.575, p<0.0001; and for time x genotype interaction: $F_{(17,136)}$=9.564, p<0.0001. **(B)** Total distance (cm) traveled in 1 hour.****p<0.0001 by a Student's t-test. **(C)** Stereotypy count (repeated beam breaks) per 5 min. F values, listed as in (A): $F_{(1,8)}$=33.93, p=0.0004; $F_{(17,136)}$=4.869, p<0.0001; and $F_{(17,136)}$=5.193, p<0.0001. **(D)** Total stereotypy count in 1

hour. ***p=0.0003 by a Student's t-test. **(E-H)** As in (A-D) in mice injected with d-amphetamine (3mg/kg i.p. at 10μl/g); n=8 wild-type, n=8 *Rhes*$^{-/-}$ mice. F values, listed as in (A): for (E) $F_{(1,14)}$=21.69, p=0.0004; $F_{(17,238)}$=28.88, p<0.0001; and $F_{(17,238)}$=9.496, p<0.0001; and for (G) $F_{(1,14)}$=25.37, p=0.0002; and $F_{(17,238)}$=3.939, p<0.0001; and $F_{(17,136)}$=11.63, p<0.0001. (F) ***p=0.0003; (H) ***p=0.0001, by a Student's t-test. **(I-L)** As in (A-D) in wild-type, *Rasgrp1*$^{-/-}$, *Rhes*$^{-/-}$, *Rhes*$^{-/-}$/*Rasgrp1*$^{-/-}$ mice upon injection of 3mg/kg d-amphetamine (i.p. at 10μl/g); n=6 wild-type, n=7. *Rasgrp1*$^{-/-}$, n=6 *Rhes*$^{-/-}$, n=6 *Rhes*$^{-/-}$/*Rasgrp1*$^{-/-}$ mice. F values, listed as in (A): for (I) $F_{(3,21)}$=30.13, p<0.0001; $F_{(17,357)}$=65.94, p<0.0001; and $F_{(51,357)}$=8.428, p<0.0001; and for (K) $F_{(3,21)}$=11.63, p=0.0001; $F_{(17,357)}$=8.980, p<0.0001;and $F_{(51,357)}$=5.545, p<0.0001. P values were (J) *p=0.049, **p=0.0019; (L) *p=0.035; n.s., not significant. **(M-P)** As in (A-D) in wild-type, *Rhes*$^{+/-}$/*Rasgrp1*$^{+/+}$, *Rhes*$^{+/-}$/*Rasgrp1*$^{+/-}$, *Rhes*$^{+/-}$/*Rasgrp1*$^{-/-}$ mice upon injection of 3mg/kg d-amphetamine (i.p. at 10μl/g); n=6 wild-type, n=8 *Rhes*$^{+/-}$/*Rasgrp1*$^{+/+}$, n=6 *Rhes*$^{+/-}$/*Rasgrp1*$^{+/-}$, n=6 *Rhes*$^{+/-}$/*Rasgrp1*$^{-/-}$ mice. F values, listed as in (A): (M) $F_{(3,22)}$=7.591, p=0.0012; $F_{(17,374)}$=22.11, p<0.0001; and $F_{(51,374)}$=3.214, p<0.0001; and for (O) $F_{(3,22)}$=11.34, p=0.0001; $F_{(17,374)}$=10.48, p<0.0001; and $F_{(51,374)}$=5.630, p<0.0001. P values were (N) **p=0.0027; (P) *p<0.026, ****p<0.0001. Data are mean ± SEM, n indicated in each panel's legend. F-values in (A, C, E, G, I, K, M, and O) were calculated by two-way repeated measures (mixed model) ANOVA followed by a *post hoc* Bonferroni multiple comparison tests. Two-way multiple comparisons were significant, but were not included in the figures to keep the presentation clean. P values in (J, L, N, and P) were calculated by one-way ANOVA followed by a *post hoc* Tukey's multiple comparison tests.

A

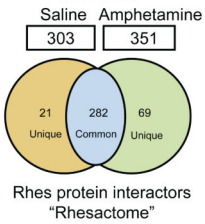

C

	Saline		Amphetamine	
Top pathways	*P* value	Overlap	*P* value	Overlap
EIF2 signaling	2.92E−33	19.30%	9.16E−45	25.30%
mTOR signaling	2.01E−09	8.30%	1.35E−13	11.60%
eIF4 and p70S6K signaling	2.24E−07	4.50%	7.35E−11	11.50%
GNRH signaling	1.22E−05	7.40%	—	
Protein kinase A signaling	—	—	1.40E×06	5.40%
Clathrin-mediated endocytosis	—	—	3.65E×06	7.10%
Top biofunctions	*P* value	Molecule	*P* value	Molecule
Cell death and survival	2.91E−03 – 2.17E−20	131	3.20E−03 – 1.96E−23	141
Cellular assembly and organization	3.34E−03 – 3.50E−20	109	3.23E−03 – 6.24E−19	122
Cellular function and maintenance	3.46E−03 – 3.50E−20	89	3.28E−03 – 6.24E−18	119
Cellular development	2.82E−03 – 8.39E−17	135	3.23E−03 – 2.13E−19	105
RNA posttranscriptional modification	—	—	7.54E−04 – 5.68E−21	39

B

"Rhesactome" in amphetamine vs saline in WT mice

Name	ID	Log_2 fold change
Peroxiredoxin-1	Prdx1	−25.37
Neural cell adhesion molecule 1	Ncam1	−24.66
Synaptotagmin-1	Syt1	−24.32
Complement C3	C3	−24.03
Neuralized-like protein 4	Neurl4	−23.72
Gamma-enolase	Eno2	−23.71
Splicing factor U2AF	U2af2	−20.98
L-Lactate dehydrogenase	Ldhb	−4.16
Guanine nucleotide-binding protein G(i) subunit α-1	Gnai1	−3.71
Catalase	Cat	−3.14
Heterogeneous nuclear ribonucleoprotein H	Hnrnph1	−3.05
Gasdermin-A	Gsdma	−2.94
Serine/threonine-protein kinase TBK1	Tbk1	−2.94
Ras-related C3 botulinum toxin substrate 1	Rac1	−2.85
Glutamate decarboxylase 1	Gad1	−2.53
Calmodulin-regulated spectrin-associated protein 2	Camsap2	−2.43
cAMP-dependent protein kinase type II-β regulatory subunit	Prkar2b	−2.42
Kinesin heavy chain isoform 5C	Kif5c	0
GTP-binding protein Rhes	Rasd2	0.1
Regulator of G protein signaling 9	Rgs9	0.34
Ras/Rap GTPase-activating protein SynGAP	Syngap1	0.41
OS, *Mus musculus*	Rbm39	1.71
Ubiquitin C-terminal hydrolase CYLD	Cyld	1.73
LanC-like protein 2	Lancl2	1.73
Zinc finger C2HC domain-containing protein 1A	Zc2hc1a	1.95
Inward rectifier potassium channel 4	Kcnj4	1.97
Myelin expression factor 2	Myef2	2.01
Laminin subunit γ-1	Lamc1	2.94
AP-3 complex subunit δ-1	Ap3d1	2.96
60*S* ribosomal protein L15	Rpl15	4.1
40*S* ribosomal protein S15a	Rps15a	4.17
Calcium uptake protein 3	Micu3	22.7
Purine-rich element-binding protein γ 1	Purg	22.71
Heterogeneous nuclear ribonucleoprotein	Hnrnph2	22.74
Plasma membrane calcium-transporting ATPase 2	Atp2b2	23.65
Neuromodulin OS	Gap43	23.65
Protein FAM126B	Fam126b	23.67
Cytochrome c oxidase subunit NDUFA4	Ndufa4	25.63
Nucleophosmin OS	Npm1	25.69
60*S* ribosomal protein L17	Rpl17	26.61
60*S* ribosomal protein L35	Rpl35	26.76
Synaptotagmin-17	Syt17	30.33

Exclusive in saline
Present in saline and amphetamine
Exclusive in amphetamine

D

"Rhesactome" enriched in amphetamine

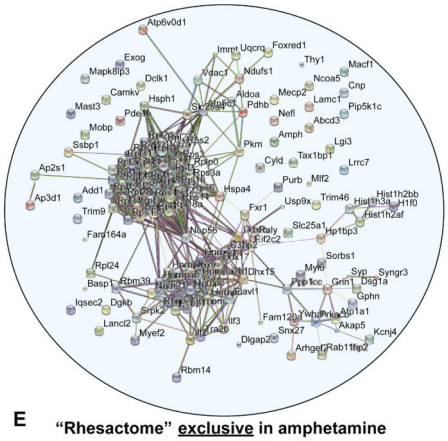

E

"Rhesactome" exclusive in amphetamine

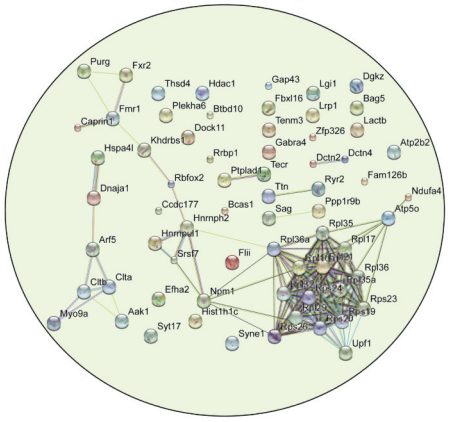

Figure 3. Amphetamine induces protein complexes of Rhes (a "Rhesactome") in the striatum

(**A**) Venn diagram of Rhes-interacting proteins "Rhesactome" in wild-type mice striatum in saline and amphetamine (3 mg/kg i.p. at 10 μl/g) conditions. (**B**) Log_2 fold change in the abundance of the indicated proteins in Rhes immunoprecipitates from lysates from wild-type mice injected with amphetamine compared to those injected with saline. (**C**) Ingenuity pathway analysis of the "Rhesactome" in saline and amphetamine conditions in wild-type mice. (**D and E**) STRING-based bioinformatics curation of the Rhesactome protein complexes enriched upon amphetamine treatment, compared to saline (D), and protein

complexes exclusively present under amphetamine conditions (E). Data are representative of n=3 IP/LC-MS/MS experiments.

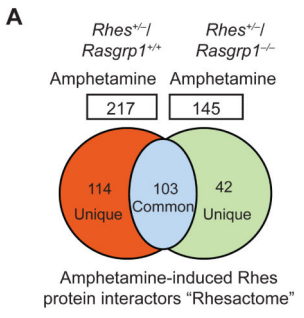

C

	Rhes+/−/Rasgrp1+/+		Rhes+/−/Rasgrp1−/−	
Top Pathways	p-value	Overlap	p-value	Overlap
EIF2 Signaling	7.21E-32	17.00%	1.12E-40	18.00%
mTOR Signaling	7.48E-09	7.00%	4.71E-12	7.50%
Regulation of eIF4 and p70S6K Signaling	3.63E-08	7.60%	6.01E-10	7.60%
Adrenergic Signaling	1.84E-04	6.90%	–	–
IL-1 Signaling	2.35E-04	6.60%	–	–
Remodeling of Epithelial Adherens Junctions	–	–	8.89E-05	7.40%
Germ Cell-Sertoli Cell Junction Signaling	–	–	1.58E+00	4.00%
Top Biofunctions	p-value	Molecule	p-value	Molecule
Cellular Assembly and Organization	5.20E-03 - 3.90E-18	86	6.63E-03 - 4.36E-09	51
Cellular Function and Maintenance	5.20E-03 - 3.90E-18	84	–	
Cell Morphology	5.20E-03 - 4.58E-18	74	6.63E-03 - 4.36E-09	44
Cellular Development	3.86E-03 - 4.58E-18	76	–	–
Cellular Growth and Proliferation	3.86E-03 - 4.58E-18	99	–	–
Gene Expression	–		5.25E-03 - 1.91E-14	36
Protein Synthesis	–		4.24E-03 - 8.77E-16	35

B

Absent			Altered			Present		
Protein ID	Rhes+/− Rasgrp1+/+	Rhes+/− Rasgrp1−/−	Protein ID	Rhes+/− Rasgrp1+/+	Rhes+/− Rasgrp1−/−	Protein ID	Rhes+/− Rasgrp1+/+	Rhes+/− Rasgrp1−/−
Ppfia3	6.52		Actn2	1.83	1.35	Dsg1a		2.44
Pde2a	4.86		Nefh	1.71	-0.2	Dlat		2
Tgm1	3.67		Thy1	1.57	-0.2	Mlf2		1.51
Actn4	3.51		G3bp2	1.53	0.33	Ncdn		1.5
Coro2b	2.88		Fxr1	1.5	1.18	Pclo		1.36
Gpr98	2.79		Epb41l3	1.42	-0.1	Tubb4a		1.18
Tnik	2.79		Hnrnpul1	1.39	0.79	Rps4x		1.06
Macf1	2.15		Gpr158	1.36	0.12	Csde1		1.04
Lrrc7	2.04		Dlgap3	1.22	0.07	Camk2a		1.01
Cacna2d1	1.99		Hnrnpc	1.22	-0.2	Slc25a11		1
Gnai1	1.99		Myo5a	1.13	-0.1	Dync1h1		0.95
Obscn	1.92		Plec	0.84	-0.3	Lactb		0.94
Bdh1	1.91		Hnrnpd	0.84	-0.5	Tuba4a		0.83
Lsamp	1.85		Myef2	0.76	-1.4	Ranbp2		0.74
Plg	1.69		Jup	0.73	0.22	Hist1h2bb		0.72
Ncam1	1.68		Mark2	0.72	0.05	Naa50		0.65
Safb	1.66		Ctnnd2	0.68	-1	Gstm5		0.64
Akap5	1.5		Rpl23a	0.63	-0.1	Rpl31		0.64
Cntn1	1.5		Rasd2	0	-0.3	Ap2m1		0.59

Log2 Fold Change
High
Low
Absent

D

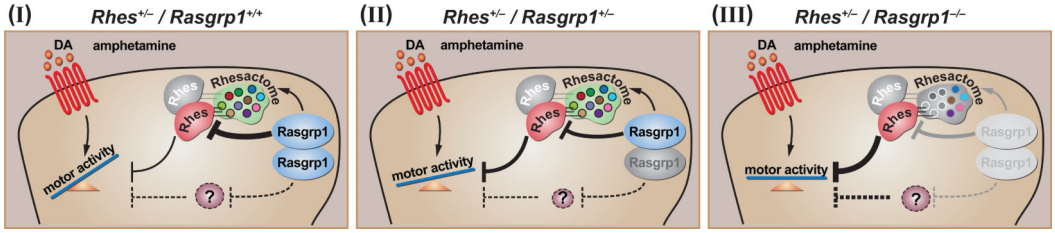

Figure 4. RasGRP1 mediates "Rhesactome" formation in the striatum

(A) Venn diagram of Rhes-interacting proteins "Rhesactome" in *Rhes*$^{+/-}$/ *Rasgrp1*$^{+/+}$ and *Rhes*$^{+/-}$/ *Rasgrp1*$^{-/-}$ mice striatum in amphetamine (3 mg/kg i.p. at 10 μl/g) condition. (**B**). Selected striatal interactors of Rhes (log_2 fold change in response to amphetamine over saline) absent, altered or present in *Rhes*$^{+/-}$/*Rasgrp1*$^{-/-}$ mice compared to *Rhes*$^{+/-}$/ *Rasgrp1*$^{+/+}$. (**C**) Ingenuity pathway analysis of the "Rhesactome" in amphetamine-njected *Rhes*$^{+/-}$/ *Rasgrp1*$^{+/+}$ and *Rhes*$^{+/-}$/ *Rasgrp1*$^{-/-}$ mice. Data are representative of n=2 IP/LC-MS/MS experiments. (**D**) Working Model, in which RasGRP1 exerts inhibitory control over

Rhes through a “Rhesactome” that prevents Rhes from inhibiting amphetamine-induced motor behavior (I). Genetic depletion of one copy or both copies of *Rasgrp1* reduces its inhibitory control over Rhes, thus enhancing Rhes-mediated inhibition of amphetamine-induced motor behavior (II), and complete genetic depletion of *Rasgrp1* forms defective “Rhesactome” enabling the highly inhibitory activity of Rhes towards amphetamine-induced motor behavior (III).